FURTHER REMARKS ON "A NEW METHOD FOR THE APPLICATION OF LUMINESCENT SCREENS TO GLASS SURFACES"[1]

WALTER H. KOHL

Research Division, Collins Radio Company, Cedar Rapids, Iowa

ABSTRACT

A process previously described by the author under the title put in quotation marks above (1) was further developed and its mechanism elucidated. It refers to the deposition of a sulfurous deposit on the inside wall of the glass envelope to be coated, comprising amorphous and/or crystalline sulfur, sulfur trioxide or a polymer thereof of the form $(S_2O_3)_x$. These deposits pick up powders in a uniform layer when the latter are caused to slide over them. When the sulfurous deposits are then driven off by external heat, the powder remains on the glass. Means for producing such phosphor screens are described and illustrated.

INTRODUCTION

In an earlier report (1), the author described a process which was used for the coating of cathode ray tube screens with phosphors, and references to it have appeared in other papers (2–5, 13) The process was extensively used by the author for many years and several refinements were incorporated during this time.[2] This information was passed on to several manufacturers during the war, but no account given in the literature of these improvements. Lately, some further work was done on this process in the laboratory with which the writer is now affiliated. For convenience, these two periods will be referred to as the "earlier period" and "recent investigations." While it has not been possible at any time to apply to the process the scrutiny in terms of experimental and theoretical analysis which would be desirable to fully analyze and interpret it, it is felt that a number of observations might be of some interest to workers in the fields of surface physics and chemistry, as well as to industrial laboratories concerned with the production of powder coated glass envelopes.

THE APPLICATION OF SULFUROUS COATINGS

For convenience of reference, the original procedure described in 1935 (1) will be briefly restated. It was found that the products of partial combustion of carbon disulfide in air produced a greenish-yellow deposit on the inside surface of a glass envelope that was held over the burning CS_2 so that the combustion products entered the envelope. When dry, free flowing powder was caused to slide over this coated surface, a uniform layer of powder was picked up and adhered to the coated surface after excess was shaken off.

[1] Manuscript received December 20, 1948. This paper prepared for delivery before the Philadelphia Meeting, May 4 to 7, 1949.

[2] The earlier work was done at Rogers Electronic Tubes, Ltd., Toronto, Ontario, Canada.

The sulfurous coating was then removed by torching the glass envelope from the outside with a bushy flame from a Bunsen burner. This caused the sulfurous vapors to escape through the open neck of the tube to the atmosphere and a uniform powder film remained in place and adhered with great tenacity against shock, but was easily wiped off with a cloth soaked in alcohol. The entire coating procedure, starting with a well-cleaned glass bulb and finishing with a screen deposit ready for sealing, should not take more than 15 minutes for a 5 in. (12.7 cm) diameter bulb. Cathode ray tube screens were usually produced by first removing the sulfurous

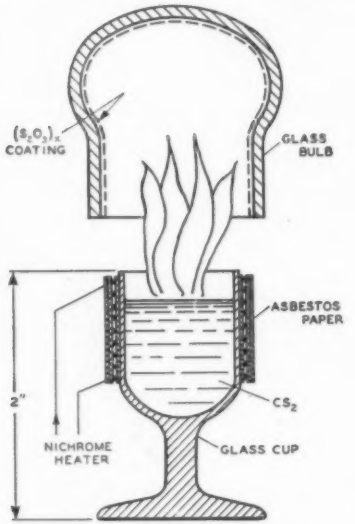

FIG. 1

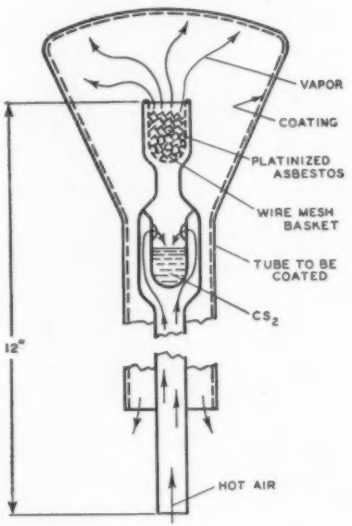

FIG. 2

FIG. 1. Application of sulfurous coating onto small glass envelope by burning CS_2 in heated glass cup.

FIG. 2. "Sulfur gun," type A, for application of sulfurous coating to larger glass envelopes.

deposit from the tube wall before the powder was introduced into the tube so that only the screen face became coated with powder. When dealing with powders that are sensitive to oxidation when heated in air, the sulfurous deposit should be driven off under a partial vacuum of the order of a few microns. The advantages of the process were speed in operation, absence of organic binders which are liable to have a deleterious affect on luminescence and finally, uniformity of the deposit obtained. As no quantitative measurements have been made on the relative merit of the process in comparison with settling techniques now commonly used in the industry for some years, the advantages quoted are not to imply that the process is necessarily better than others. Such matters as contrast, secondary emission, and effects on color would have to be investigated quantitatively.

The fact remains, however, that oscilloscopes made with screens after this process operated very satisfactorily for many thousands of hours.

In order to suit different requirements, a number of "vapor-guns" were designed during the earlier period and these are shown in diagrammatic form in Fig. 1, 2, 3, 4. The small glass bowl shown in Fig. 1, wrapped with asbestos paper on which a few turns of No. 28 Nichrome wire are wound to serve as a heater, works very well for coating small envelopes such as receiving tube blanks. Just enough heat is supplied to have the CS_2 simmer slightly and burn with its characteristic blue flame.[3]

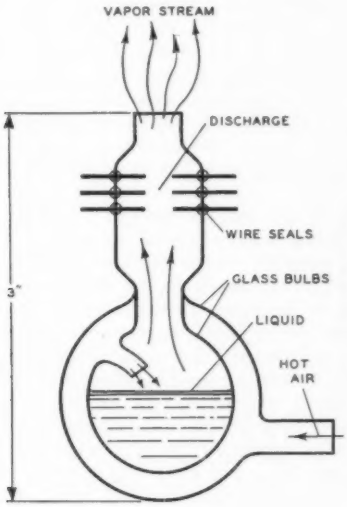

FIG. 3

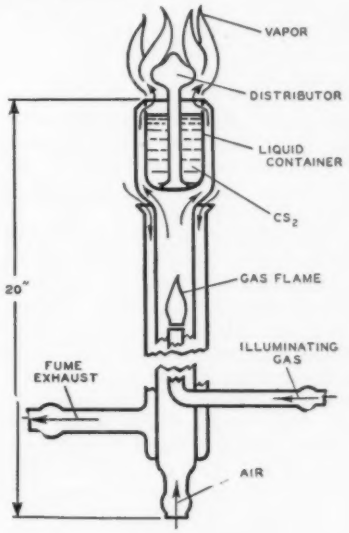

FIG. 4

FIG. 3. The aerosol generator described by Professor Regener (6)

FIG. 4. "Sulfur gun," type B, for the application of sulfurous coating to large glass envelopes.

In order to coat larger envelopes and especially pear-shaped bulbs with a screen diameter of about 4 in. (10.2 cm) diameter, the gun type A shown in Fig. 2 is useful. It becomes necessary to supply auxiliary air and heat to the CS_2 within the blank to be coated, and this is readily achieved by using hot air for both purposes. This design was used by Professor Regener for the production of aerosols from volatile liquids and is described in the literature (6). His original form is shown in Fig. 3. It was adopted by the present author for his special purpose in December, 1937, and found to work very well. In order to facilitate the condensation of vapor, Regener

[3] Sulfurous vapors are, of course, very objectionable to the operator, and provisions must be made to dispose of them. The coating should thus either be done under a fume hood or, in the absence of such facilities, the vapors should be drawn off by a water jet pump.

used a spark discharge between the sealed-in wires, and it does indeed speed up the formation of vapor. This "Regener Gun" was used later without the discharge quite satisfactorily, especially when it was found that the insertion of platinized asbestos served the same purpose much better.

The coating of large envelopes was for a long time very unreliable. It might work out to perfection one day and not at all on another, or even later during the same day. Only when it occurred to the author to correlate humidity data (from the weather bureau) with his failures over a prolonged period, was it realized that high humidity was essential to the success of the process when coating large envelopes. It was thus necessary to provide water vapor under controlled conditions. This was achieved by introducing a small gas flame below the CS_2 container as shown in Fig. 4. As city illuminating gas contains 40–50 per cent of hydrogen by volume, this burns into water and provides the necessary moisture which favors the formation of SO_3. At the same time, the gas flame heats the CS_2 container so that air at room temperature, rather than hot air, can be fed to this gun, type B. This improvement was made in August, 1936, and put the process on a more reliable basis.

The design of the gun shown in Fig. 4 will now be readily understood. Of the three concentric glass tubes, the inner one leads to the gas jet, the intermediate one feeds air under slight pressure to the gas flame and heat and moisture are conveyed around the CS_2 container to the mouth at the top where it is supported on 3 dimples in the glass. The outer tube draws off the sulfurous vapors and, by the suction created, increases turbulence of the vapors within the envelope to be coated. The mushroom-shaped glass part marked "distributor," which stands in the CS_2 container, protects the center of the screen from direct impact of the vapors. When working under a fume hood, the outermost tube can be dispensed with. When using the jet pump for suction, the whole gun is supported within the neck of the tube to be coated by means of a split cork ring so as to seal off the interior of the envelope from the outside atmosphere.

As mentioned above, the powder may be fed into the coated bulb immediately after the sulfurous coating has been produced, or, for reasons of economy, the sulfurous coating may be wiped off from areas where no powder deposit is desired and the powder brought into contact with the screen area thereafter. The manner in which the powder is best fed into the bulb depends on the physical state of the powder. Some powders require very little precaution and may be passed into the tube from a piece of filter paper or the like. When the powder reaches the precoated area, the tube is rotated so that the powder slides over it and is picked up uniformly without streaks. The excess powder is then shaken off and poured out for further use. Many powders do not lend themselves to this simple procedure, as they leave streaky deposits when thus used, and this behavior is closely connected with their particle size distribution. An average particle size of the order of 5 microns works very well, but larger grained powders (20 microns) require special treatment. The electrical charge acquired by the powder while sliding over the coated glass also may have a bearing on the mechanism of pick-up. It has been shown (7) that the magnitude of the charge developed on dust particles of the size range 1–50 microns when

sliding over a wall, coated with the same material, is related to the size of the particles. In the 'sulfur process"[4] the particles are not originally the same as the coating on the wall, but become so after a first deposit is formed.

It is also interesting, in this connection, that when, at one time, luminescent powder was slid into a "vapor coated" bulb and allowed to rest at one spot on the screen for 24 hours before the bulb was rotated and the powder thus distributed over the screen area, a blank area resulted on the screen where the powder had been resting. This experiment was recently repeated with the same result using Patterson Phosphor 608 (Zn_2SiO_4:Mn). The remainder of the screen was coated satisfactorily. It has also been

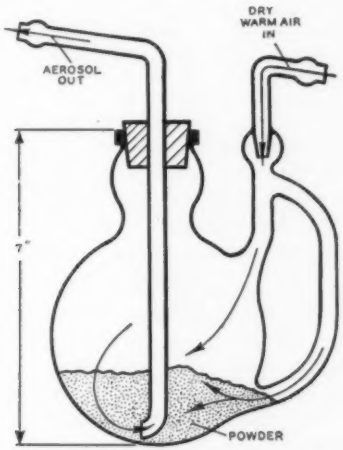

FIG. 5. Powder gun for dispersion of phosphors in the air stream

observed that powders deposit more readily after sliding over the clean glass wall than when sliding through a brass tube before landing on the screen area.

A powder gun developed by the writer is shown in Fig. 5. It lends itself well to the production of an aerosol which is blown from its mouth into the tube to be coated and results in uniform deposits of powders which tend to give streaky deposits on simple sliding contact in bulk. It may sometimes be necessary to build up the thickness of the screen by depositing a second sulfurous coating onto the first powder layer and then follow with another powder deposit. In such cases only one final torching is required to remove the several sulfurous deposits. The introduction of steam from a steam generator terminating in a vertical tube that is inserted into the bulb to be coated between the individual coating operations is often helpful.

The possibility of producing multilayer screens by this process consisting

[4] This term is used for brevity and does not imply that sulfur is the only constituent of the deposit obtained from it.

of several different types of powder was first explored by the author in May, 1938, with the objective of producing screens of long delay. It is known from the literature on this subject that phosphorescence of long duration is more readily obtained by photoexcitation (photoluminescence) than by electron impact excitation (cathodoluminescence). This condition can be realized in a cathode ray tube by depositing on the glass first a layer of a long-delay phosphor which in turn is covered by a second screen layer facing the cathode. The second layer is excited by electron bombardment to emit radiation in the ultraviolet region of the spectrum, and this radiation in turn will excite the layer adjacent to it in the visible range of the spectrum with long delay times, depending on its composition.

Such multilayer or "cascade screens" have found widespread use during the last war in radar scopes which had a (Zn, Cd)S:Cu layer on the glass and a ZnS:Ag coating facing the electron beam. Afterglow periods of ½ hour have been reported from such screens (8). Long-delay screens of this type were developed by R.C.A. in collaboration with M.I.T. under Contract OEM-sr-441 for the Office of Scientific Research and Development. They became known as P7 and P14 screens, and some of their characteristics and methods of measuring them were recently described (9). These screens were settled from liquid suspensions of the phosphors. The "sulfur process" is naturally applicable to the coating of fluorescent lamps and this was demonstrated by the author in 1935.

CHEMISTRY OF THE "SULFUR PROCESS"

In order to come to some conclusions on the chemical aspects of the "Sulfur Process," the following reactions suggest themselves as likely to occur:

$$\text{Reaction I:} \quad 2CS_2 + 5O_2 = 2CO + 4SO_2$$
$$\text{Reaction II:} \quad CS_2 + 3O_2 = CO_2 + 2SO_2$$
$$\text{Reaction III:} \quad 2CO + SO_2 = S + 2CO_2$$

and from I + III combined:

$$2CS_2 + 5O_2 = 2CO_2 + S + 3SO_2$$

A small amount of CS_2 vapor will remain as such (10) and some SO_2 will enter from the presence of city gas flames when using Gun B (Fig. 4). From the same source, considerable water vapor is introduced which in the presence of a catalyst will favor the formation of SO_3 from SO_2:

$$2SO_2 + O_2 = 2SO_3$$

This reaction is reversible and, for the case of platinized asbestos acting as catalyst, takes place at a maximum rate to the right at a temperature near 410 C(11) when it is exothermic.

It has also been reported (12) that SO_3 dissolved in SO_2 polymerizes to a firm and elastic surface skin. The presence of a greenish solid on the walls of containers used for the catalytic production of sulfuric acid may be this polymer for which a formula $(S_2O_3)_x$ has been suggested. Some of the yellow solid solution of S in $(SO_3)_x$ may also be present.[5]

The experience of the writer indicates that two types of deposits are ob-

[5] Personal comment by Professor Geo. Glockler, State University of Iowa, Iowa City.

tained in succession under favorable conditions, i.e., first a whitish deposit, followed by the greenish-yellow deposit. Under unfavorable conditions, the whitish deposit only appears and this is not as suitable to screen application as the greenish-yellow deposit.

The chemistry of sulfur in its many modifications is rather involved and no clear-cut statements can be made without more elaborate investigations for which time and facilities are not available now. However, in order to shed some light on the factors involved in the process, at least qualitatively, the following experiments were recently performed:

Experiment No. 1. Two glass bulbs in a horizontal position were connected by a glass tube from which a T-joint led to a stop cock and an aspirator pump. One bulb contained some flour of sulfur. When the pressure in the vessels was reduced to 25 mm Hg and the bulb with the sulfur heated to 450 C, sulfur sublimate condensed in the other bulb forming first a whitish tacky coating and then a yellow layer on top of it. The first coating is not soluble in CS_2, H_2O, H_2SO_4, and hot Na(OH), and is thus amorphous sulfur. The second yellow deposit is soluble in CS_2 and thus represents α or β-sulfur. The first insoluble layer takes on a yellowish tinge and greater thickness when the temperature of the bulb containing the flour of sulfur is raised to near 550 C. When the same experiment at 450 C is performed at atmospheric pressure, only a yellowish tacky non-soluble deposit is obtained, pointing again to amorphous sulfur.

Experiment No. 2. Burning CS_2 in a small container and collecting the products of combustion in a glass bulb above it at atmospheric pressure produces a yellowish, very tacky deposit which is insoluble in all reagents mentioned above and thus consists mainly of amorphous S.

Experiment No. 3. Decomposing sodium thiosulfate by the application of heat at 50 C in a set-up much like that for experiment No. 2 produces a white deposit of SO_3 according to

$$Na_2S_2O_3 \rightarrow SO_3 + Na_2S$$

The deposit decomposes in H_2O and is soluble in H_2SO_4 and insoluble in CS_2 as expected. Phosphor powder was applied to this SO_3 deposit by sliding it over the layer as in all other experiments. It adhered quite well after the SO_3 was driven off by heating the bulb in air to about 50 C.

Experiment No. 4. This set-up aimed at the production of sulfur according to the reaction

$$SO_2 + 2H_2 \rightarrow S + 2H_2O$$

when carried out in an iron pipe at red heat. A $\frac{5}{8}$ in. (1.6 cm) diameter iron pipe 2 ft (61 cm) long was mounted horizontally within a fire brick tunnel from the wall of which a blast burner protruded at one side at an acute angle to the pipe. Joined to this pipe outside the furnace enclosure to the right was a T-section of iron pipe through which SO_2 and H_2 entered respectively. Both gases were passed through 80 per cent H_2SO_4 and drawn from commercial steel tanks. At the left end of the horizontal pipe an elbow was joined to the pipe ending in a 3 in. (7.6 cm) vertical chimney of the same diameter over which glass bulbs were held to collect the reaction products. Iron chips were given into the pipe near the burner position to act as catalyst. Depending on the temperature of operation and the ratio of

gas composition fed in, white, brownish-white, and bluish vapors were obtained which, however, were not distinguishable in color when the deposit was formed on the inside of the glass bulb. The white vapors form first, in a temperature range from 850–915 C (measured by an optical pyrometer on the outside of the hot pipe). The deposit indicates SO_3 as it is soluble in H_2O and in H_2SO_4, but not in CS_2. At 950 C the brownish vapors turn into bluish vapors when the H_2 flow is increased so that the ratio H_2:SO_2 is greater than 2. Deposits obtained at this stage are very suitable for powder deposition. They are composed of sulfur soluble in CS_2 and will combine with Hg to form black HgS.

Experiment No. 5. Using the setup of experiment No. 4, but feeding dry SO_2 and O_2, one obtains an abundance of white vapors of SO_3 with Fe_2O_3 acting as catalyst. The deposits react with H_2O and are soluble in H_2SO_4 but not in CS_2. Powder deposits can again be produced.

Experiment No. 6. By filling a bulb with H_2S and igniting at the open mouth, one again obtains two types of deposits, of which one is soluble S and the other insoluble S.

SUMMARY AND CONCLUSIONS

The conclusions that may safely be drawn from these experiments together with the performance of the various guns described above are the following. A variety of sulfurous deposits lend themselves to the deposition of powder screens. Amorphous sulfur, crystalline sulfur, sulfur trioxide, and sulfur sesquioxide polymer $(S_2O_3)_x$, in combination or separately, when freshly condensed on a glass surface, have the property of picking up powder layers when brought in contact therewith. When these sulfurous elements or compounds are driven off by the application of heat, their effect on the surface is such that the powder layers are retained on the glass. A combination of several of the sulfur type coatings rather than only one seems to act more favorably.

These layers can be produced in a variety of ways and one of the more obvious methods would be to replace CS_2 as a source by a gun fed directly with suitable gases which combine in the presence of a catalyst to produce the desired deposit. Such an arrangement would be more applicable to routine production and eliminate the need for handling the poisonous liquid CS_2. One such gun under study at present comprises two concentric metal tubes fed, respectively, with SO_2 and O_2 from steel containers and carrying at the top a porous ceramic plug which has deposited in its pores active catalyst. This will produce SO_3, when the temperature of the plug is controlled to suit the optimum conversion yield. By feeding SO_2 and H_2 to such a gun, sulfur deposits can be obtained, and by proper combination of the use of two such guns to which the bulbs are exposed in succession, any suitable deposit can be obtained. These simplified guns are now under development and may be reported on later. The possibility also remains that deposits other than those containing sulfur could be used in a similar manner.

ACKNOWLEDGEMENT

J. O. Barlon and George Pixley of this laboratory constructed the apparatus and performed all the tests. Their untiring efforts are gratefully

acknowledged. Thanks are due to the management of the Collins Research Laboratory who permitted the further investigation of the process and to Professor Geo. Glockler of the State University of Iowa for several helpful discussions.

Any discussion of this paper will appear in the discussion section of Volume 96 of the TRANSACTIONS of the Society.

REFERENCES

1. *Can. J. Research A*, **13**, 126–132 (1935).
2. HENRY W. PARKER, U. S. Pat. 2,094,242, Sept. 28, 1937.
3. HENRY W. PARKER (To Rogers Radio Tubes, Ltd.) Can. Pat. 373,072, Apr. 12, 1938.
4. *Communications*, p. 24, Jan. (1938).
5. C. H. BACHMAN, "Techniques in Experimental Electronics," p. 205, John Wiley & Sons, Inc. (1948).
6. FREUNDLICH, "Kapillarchemie," p. 1068, Leipzig (1923).
7. J. W. Hansen, *Bull. Am. Phys. Soc.*, **22**, 7, July (1947).
8. *Electronics*, pp. 126–130, Feb. (1948).
9. R. E. JOHNSON AND A. E. HARDY, *R.C.A. Rev.*, **8**, 660–681, Dec. (1947).
10. *Ind. Eng. Chem.*, **11**, 130–133 (1919).
11. R. D. MILES, "Manufacture of Sulphuric Acid," p. 28 Guerney and Jackson, London (1925).
12. H. GERDING, *Naturwissenschaften*, **25**, 251 (1937).
13. MEIER SADOWSKY, *J.* (*and Trans.*) *Electrochem. Soc.*, **95**, 112–128 (1949).

BISMUTH AS ACTIVATOR IN FLUORESCENT SOLIDS[1]

F. A. KROEGER, J. TH. G. OVERBEEK, J. GOORISSEN, AND J. VAN DEN BOOMGAARD

Philips Research Laboratories, Eindhoven, Holland

ABSTRACT

Trivalent bismuth forms fluorescence centers in its own compounds as well as in other systems in which it is present as an activator. The fluorescent emission consists of various bands lying between the ultraviolet and the red end of the spectrum. The relative intensity of these bands depends upon the nature of the host lattice and the temperature of observation.

Sulfates and phosphates of the alkaline earth group show predominantly red fluorescence. The red fluorescence of $Ca_2P_2O_7$:Bi shows the remarkable feature that its temperature dependence is different for excitation by cathode rays and by x-rays.

INTRODUCTION

Bismuth is known to be responsible for fluorescence in its own compounds as well as in other systems containing it as an activator. Wiedemann and Schmidt (1) describe a blue fluorescence of Bi_2O_3, and Randall (2) mentions a blue fluorescence of $BiCl_3$ at liquid air temperature. The activating properties of bismuth in foreign materials have been studied with the oxides, sulfides, and selenides of calcium, strontium, and barium (3–6), with aluminum oxide in which it produces a blue (7) or a red and blue (8) cathodofluorescence, with alkali halides (9), with tungstates and molybdates in which it produces yellow fluorescence (10–13), and with sulfates of the alkaline earth metals in which it produces a red cathodofluorescence (14). Finally, phosphate glasses containing bismuth show a bluish white fluorescence upon excitation by short wave ultraviolet (15).

In a preliminary investigation we prepared a number of oxides, phosphates, sulfates, silicates, and aluminates activated with bismuth. These products were prepared either by coprecipitation of the base material with the corresponding bismuth compound, followed by heating in a suitable atmosphere, or by mixing oxides, nitrates, carbonates, or other easily decomposed compounds and heating them at a temperature sufficiently high to assure reaction. A number of them showed cathodofluorescence at room temperature. Most phosphors that were not responsive fluoresced when cooled to lower temperatures. In all cases the fluorescence varied between blue, yellow, and red. The chemical and physical properties of some of the most interesting systems will be reported in this paper.

PURE BISMUTH COMPOUNDS

Pure Bi_2O_3 and $BiPO_4$ both show fluorescence upon excitation by λ 2537, x-rays, or cathode rays, at low temperatures. The emission of Bi_2O_3 consists of two bands, one in the blue with a maximum at 3900 Å and the

[1] Manuscript received March 7, 1949. This paper prepared for delivery before the Philadelphia Meeting, May 4 to 7, 1949.

other in the yellow. The latter is too weak to be measured accurately. The emission of $BiPO_4$ is white-blue with a maximum at 4200 Å (Fig. 1). Both materials show strong absorption of ultraviolet radiation below 3500 Å. Exact absorption measurements are difficult because radiation which is absorbed also causes some visible blackening of the material. Approximate reflection spectra are indicated in Fig. 1.

$AlPO_4$, $LaPO_4$, AND La_2O_3 PHOSPHORS

Lanthanum phosphate activated with $3 \cdot 10^{-2}$ moles $BiPO_4$ per mole $LaPO_4$ shows a strong blue fluorescent band with a maximum at 4400 Å;

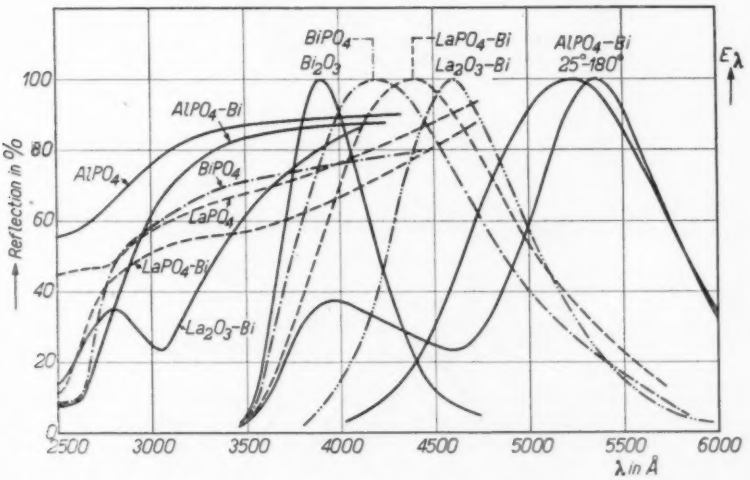

FIG. 1. Spectral distribution of the diffuse reflection and of the fluorescence, for Bi_2O_3, $BiPO_4$, $LaPO_4$:$3 \cdot 10^{-2}$ $BiPO_4$, La_2O_3:10^{-2} Bi_2O_3, and $AlPO_4$:10^{-2} $BiPO_4$. The reflection for unactivated $LaPO_4$ and $AlPO_4$ is also shown. The curves are for excitation by λ 2537 at −180 C., for $AlPO_4$:Bi also at room temperature.

lanthanum oxide with 10^{-2} moles Bi_2O_3 per mole La_2O_3 shows blue fluorescence with a maximum at 4600 Å; $AlPO_4$ with 10^{-2} moles $BiPO_4$ shows fluorescence in two bands, one at 3950 Å and another more intense one with a maximum at 5350 Å at −180 C, or 5180 Å at 25 C. The activator concentrations listed represent amounts close to the optimum for maximum intensity of fluorescence.

The pure base materials absorb only weakly in the ultraviolet, but the activated products do show strong absorption. Irradiation in these absorption bands leads to fluorescence. Absorption and emission bands are shown in Fig. 1. Fig. 2 shows the temperature dependence of the fluorescence, indicating the usual loss of efficiency with increasing temperature. The weak slope in the curve for $AlPO_4$:Bi below room temperature is due

to quenching of the blue band; the steep portion above room temperature indicates the quenching of the green band.

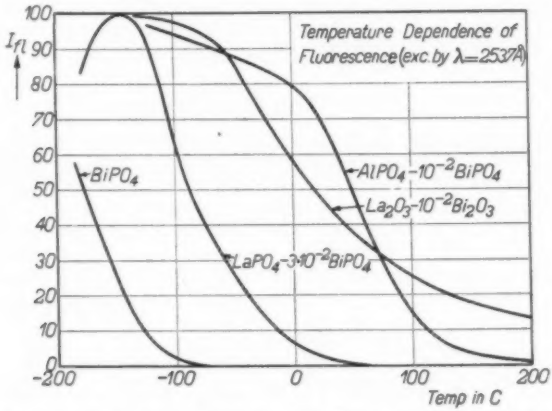

FIG. 2. Temperature dependence of the intensity of fluorescence of La_2O_3:10^{-2} Bi_2O_3, $LaPO_4$:$3{\cdot}10^{-2}$ $BiPO_4$, and $AlPO_4$:10^{-2} $BiPO_4$, for excitation by λ 2537.

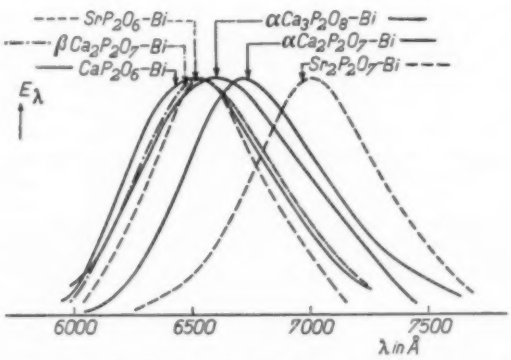

FIG. 3. Spectral distribution of the cathodofluorescence of α and β $Ca_2P_2O_7$, CaP_2O_6, $Sr_2P_2O_7$, SrP_2O_6, and $Ca_3(PO_4)_2$, all activated with 10^{-3} gram atoms Bi per mole.

PHOSPHATES OF THE ALKALINE EARTH METALS

Phosphates of calcium, strontium, and barium, activated with bismuth, were prepared by heating a mixture of the respective carbonates with ammonium phosphate. The completion of the solid state reaction and the crystal structure of the products were followed by means of x-ray diffraction patterns.

The meta- and pyro- phosphates of calcium and strontium show strong red cathodofluorescence; the orthophosphates of these elements show a similar but much weaker fluorescence, while the phosphates of barium did not fluoresce.

The spectral distributions of the most intense bands are shown in Fig. 3. The calcium pyrophosphates show different peaks depending upon the temperature of their preparation, i.e., above or below 1150 C. The difference in emission is related to a change in crystal structure from the α to the β modification. Our value for the transition point agrees with that reported by Troemel and Moeller (16).[2] A similar difference in peak positions is also found in the cathodofluorescence of the calcium pyrophosphates activated with manganese (Fig. 4).

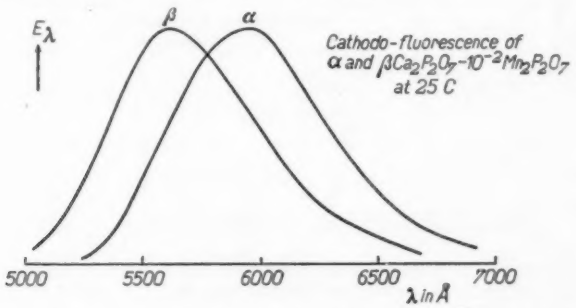

FIG. 4. Spectral distribution of the cathodofluorescence of α and β $Ca_2P_2O_7$ activated with 10^{-2} moles $Mn_2P_2O_7$.

Incorporation of bismuth produces an absorption band in the ultraviolet range which is not found in the pure base materials (Fig. 5). Even though absorption in this band is strong, it does not lead to fluorescence, whereas excitation by cathode rays does lead to strong red emission. To explain this, it is assumed that two types of centers are involved and that the absorption band is mainly due to centers which are not fluorescent at room temperature. This is demonstrated by the fact that products excited by λ 2537 at liquid air temperature do develop a new ultraviolet fluorescence emission with a peak at 3180 Å, a d also a weak blue band with maximum at 3980 Å (Fig. 5).

The red fluorescence is also excited by x-rays. The optimum concentration of bismuth is about 10^{-3} gram-atoms Bi/mole, for x-ray as well as for cathode ray excitation (Fig. 6). The x-rays for this experiment were produced with a 60 kv Philips Practix tube and a filter of 1 mm Al. This gave a continuous spectrum from about 0.2 to 1 Å with a maximum intensity at about 0.3 to 0.4 Å. The intensity was 500 roentgens per minute.

The temperature dependence of the red emission excited by 6 kv cathode rays shows a remarkable difference from that excited by x-rays. Fig. 7 demonstrates this effect for β $Ca_2P_2O_7$:$3 \cdot 10^{-3}$ Bi. The cathodofluorescence

[2] Bale, Bonner, and Hodge (17) report a transition point at 1270 C. This discrepancy may be due either to deviations from stoichiometry or to contaminations.

is nearly constant and of low intensity at low temperatures. From 0 to 150 C it increases strongly to reach a value about five times as high in intensity. It then levels off again and will probably be quenched at some temperature well above 300 C. On the other hand, the fluorescence excited by x-rays is constant over the entire temperature range. This constitutes

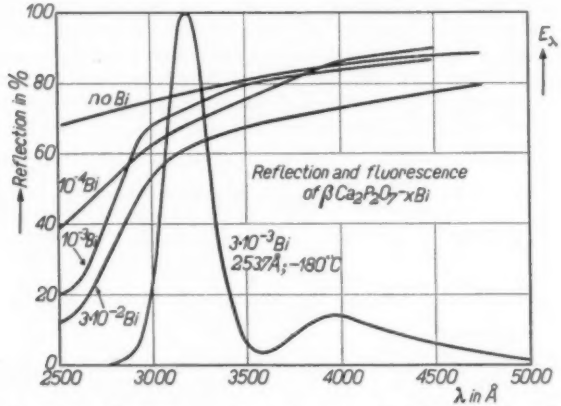

FIG. 5. Spectral distribution of the reflection of β $Ca_2P_2O_7$ containing various concentrations of bismuth, and of the fluorescence excited by λ 2537 at −180 C.

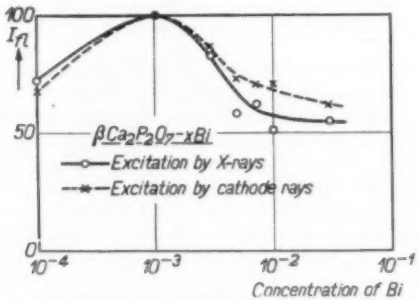

FIG. 6. Intensity of the red fluorescence of β $Ca_2P_2O_7$:Bi as a function of the bismuth concentration, for excitation by 6 kv cathode rays and 60 kv x-rays (continuous spectrum with a maximum at 0.3 to 0.4 A).

the first case, of which we know, where such a marked difference occurs between the properties of the same fluorescence excited by x-rays and by cathode rays, respectively. This is of interest because the mechanism of excitation by these two agents is usually considered to be similar.

The difference is not due to an accumulation of charge on the phosphor in the case of cathode ray excitation. Exactly the same results were obtained with cathode rays of 20 kv, which proves that the difference is not

due to a surface layer of different properties. All measurements were carried out with a stationary electron beam of about 2 μ amp/cm^2.

The difference might be explained with the assumption that the x-rays excite most of the centers directly, whereas excitation by cathode rays gives rise mainly to excited states in the base lattice, and to only a small number of directly excited bismuth atoms.

The directly excited centers produce a fluorescent emission which is independent of temperature (as long as characteristic quenching in the centers does not occur). The temperature-independent fluorescence excited by x-rays is then comparable with that excited by cathode rays at temperatures below 0 C. The main part of the cathodofluorescence,

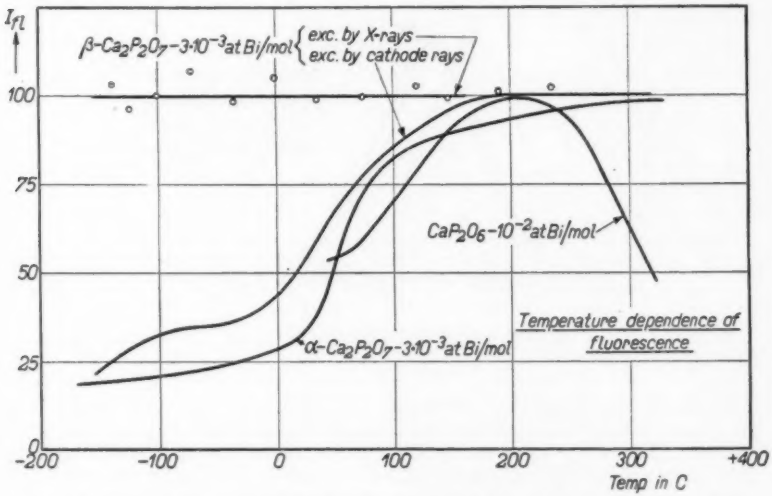

FIG. 7. Temperature dependence of fluorescence of calcium phosphates activated with bismuth, for excitation by 6 kv cathode rays and 60 kv x-rays.

however, requires the transfer of excitation energy from the lattice to the centers. If this process requires an activation energy, most of the excitation energy is lost without emission of light, at low temperatures. At a certain higher and critical temperature, the transfer process gains in prominence and the intensity of fluorescence increases. Similar effects have been observed with other systems in which the state reached in excitation is different from the state which leads to fluorescence ($Cd_2B_2O_5$:Mn, $CdSiO_3$:Mn) (18).

This explanation, however, is not fully satifactory. In the first place, bismuth does not show exceptionally strong absorption for x-rays of the wavelengths used. Furthermore, the temperature dependence for excitation by x-rays does not show even a slight increase, and the optimum bismuth concentration for x-ray excitation is not observed to be higher than

it is for cathode ray excitation, as it would be expected to be. Therefore, this point is still open to question.

Fig. 7 also shows the temperature dependence for α $Ca_2P_2O_7$:Bi and for CaP_2O_6:Bi. It proves to be similar to that for β $Ca_2P_2O_7$:Bi. With CaP_2O_6:Bi, the high temperature quenching range falls within our measuring region, the decrease setting in at 200 C.

SULFATES OF THE ALKALINE EARTH METALS

Sulfates of calcium, strontium, barium, magnesium, and zinc, activated with bismuth, were prepared by coprecipitation from solutions of the nitrates with sulfuric acid, or by evaporation of sulfate solutions. The filtered, washed, and dried materials were heated between 700 and 900 C.

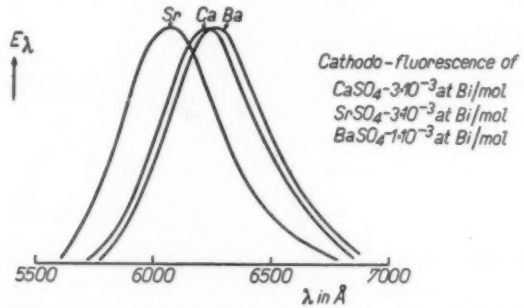

FIG. 8. Spectral distribution of the cathodofluorescence of bismuth activated $CaSO_4$, $SrSO_4$, and $BaSO_4$.

If the firing was carried out in atmospheres of air, nitrogen, or oxygen, the products turned out grayish, particularly so at high concentrations of bismuth. This color is probably due to decomposition of bismuth sulfate with formation of basic compounds. The discoloration is prevented if the firing is carried out in an atmosphere containing SO_3 such as is obtained by passing air through hot sulfuric acid. A mixture of SO_2 and O_2 may also be used.

The sulfates of calcium, strontium, and barium show a red emission upon excitation by cathode rays, x-rays, or ultraviolet. Fig. 8 shows the spectral distributions. The peaks are found to be at 6220, 6070, and 6270 Å in reasonably good agreement with the observations of L. de Boisbaudran (14) who reports the values 6180, 5980, and 6220 Å. The pure sulfates do not absorb in the near ultraviolet. Incorporation of bismuth produces an absorption band below 3600 Å which increases in intensity with the concentration of Bi. It is this absorption which is responsible for the excitation by λ 2537.

For the various forms of excitation, the intensity of fluorescence depends upon the bismuth concentration in a different manner. For excitation with x-rays or cathode rays, the intensity increases with increasing bismuth content up to about $5 \cdot 10^{-3}$ gram atoms Bi per mole sulfate. It then remains practically constant up to $3 \cdot 10^{-2}$ gram atoms Bi per mole sulfate or

higher. For excitation by λ 2537, there is an optimum concentration at 10^{-3} gram atoms Bi per mole sulfate. Above this concentration the intensity decreases rapidly. The efficiency of the ultraviolet-excited fluorescence is extremely low, even at the optimum.

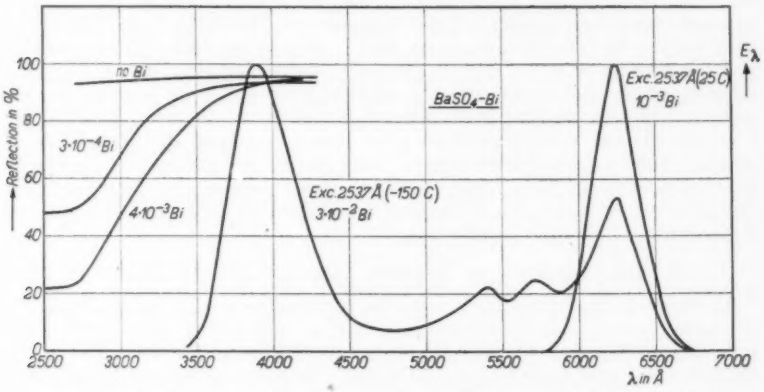

FIG. 9. Reflection of $BaSO_4$ with various concentrations of $Bi_2(SO_4)_3$. Emission of $BaSO_4$:$3 \cdot 10^{-3}$ gram atoms Bi/mole, excited by λ 2537 at room temperature, and of $BaSO_4$:$3 \cdot 10^{-2}$ gram atoms Bi/mole excited by λ 2537 at −150 C.

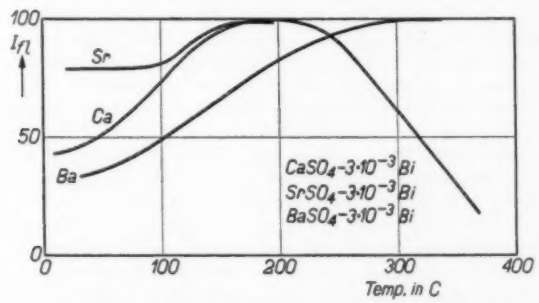

FIG. 10. Temperature dependence of the emission of $CaSO_4$, $SrSO_4$, and $BaSO_4$ activated with $3 \cdot 10^{-3}$ gram atoms Bi/mole and excited with 6 kv cathode rays.

These properties indicate that, in addition to the centers responsible for the red fluorescence, the systems contain nonfluorescent centers which absorb ultraviolet strongly and which increase in relative concentration with increasing bismuth content. The presence of such centers is directly proven by the fluorescence of the sulfates at low temperatures: a product with $3 \cdot 10^{-2}$ Bi which is only faintly luminescent at room temperature changes its emission upon cooling to liquid air temperature. It then shows two weak bands in the green and yellow region at 5400 and 5710 Å, re-

spectively, and one strong band in the violet at 3900 Å, in addition to the normal red band (Fig. 9).

The temperature dependence of the intensity of the red cathodofluorescence is shown in Fig. 10. As with the phosphates, the intensity increases with increasing temperature up to a constant value. With $CaSO_4$:Bi, the intensity decreases above 200 C owing to temperature quenching. The measurements were hindered by strong electron "burning," particularly so with $BaSO_4$:Bi. The burning is evident only as a decrease of the intensity of fluorescence; it is not accompanied by a discoloration of the material. Heating above 200 C restores the original state so far as burning is concerned. When the heating is carried out in a vacuum, however, a new effect is observed: the substance turns gray due to thermal decomposition of bismuth sulfate as discussed above. The two effects are readily separated because electron burning appears only at those spots where electrons reach the powder, whereas the discoloration occurs over the entire area, independently of electron bombardment.

THE VALENCY OF BISMUTH ACTING AS ACTIVATOR

As shown in the introduction and in the work reported above, bismuth produces fluorescence in a large number of substances, even in its own compounds. We are therefore inclined to attribute the fluorescence to characteristic electronic transitions in the configuration formed by bismuth and its nearest neighbors.

The appearance of violet, green, yellow, and red bands might be explained in two ways. For example, it may be due to bismuth atoms of different valencies. Bismuth occurs normally in the trivalent state, but pentavalent bismuth is also known (as in sodium bismuthate). Even though the free energy of pentavalent bismuth is rather large in its pure compounds, it may well be stabilized by incorporation in suitable host lattices, such as sulfates or phosphates. A second explanation would be that the fluorescence centers are formed only by trivalent bismuth and that variations in emission are due to the influence of the lattice fields on the energy levels of the Bi^{3+} ions. Such effects may reach considerable magnitude, as is shown with the corresponding case of divalent manganese, the fluorescence of which varies from green to infrared.

In order to determine whether or not different states of valence are involved, we have analyzed a few samples of red fluorescing $Ca_2P_2O_7$:Bi which was shown to contain ultraviolet emission centers (Fig. 5). To this end, about one gram of phosphor was dissolved in hydrochloric acid which had previously been freed from oxygen by passing a current of pure nitrogen through it, and which contained some KI and a few drops of a fresh solution of starch. If the products had contained pentavalent bismuth, the latter would have formed free iodine. However, no trace of a blue color was observed. In a variation of this test, the phosphors were dissolved in hydrochloric acid. A current of pure nitrogen passed through the liquid to carry liberated chlorine, if any, into an absorption vessel with a solution of KI, H_2SO_4, and starch. Again, the tests were negative. We, therefore, feel justified in our conclusion that the fluorescent effects observed are not due to bismuth atoms of different valencies, but to trivalent bismuth in different surroundings, as outlined above.

It remains to be seen what differences in surroundings would be necessary in order to cause a variation in emission ranging from blue to red, particularly in lattices which make both bands appear. The blue and ultraviolet bands of $Ca_2P_2O_7$:Bi, $BaSO_4$:Bi, and La_2O_3:Bi are situated close to the absorption bands due to bismuth. They must be attributed to corresponding electronic transitions from the ground state to an excited state and vice versa. The red bands in the phosphates and sulfates, on the other hand, are far removed from these ultraviolet absorption bands. Absorption bands in the visible which might lead to red fluorescence have not been found. This indicates that the fluorescence must be attributed to an electronic transition between two excited states, the lower one being so high that it is not occupied at normal temperatures.

The same reasoning applies to the blue bands in the other systems, which are so widely separated from the absorption bands that the shift can not be accounted for on the basis of the Franck-Condon principle.

ACKNOWLEDGMENT

The authors wish to express their thanks to Dr. H. C. Froelich for applying numerous editorial improvements to the manuscript.

Any discussion of this paper will appear in the discussion section of Volume 96 of the TRANSACTIONS of the Society.

REFERENCES

1. E. WIEDEMANN AND G. C. SCHMIDT, *Wied. Ann.*, **56**, 201 (1895).
2. J. T. RANDALL, *Nature*, **142**, 113 (1938).
3. E. TIEDE AND GOLDSCHMIDT, *Ber.*, **62**, 758 (1928).
4. O. SCHELLENBERG, *Ann. phys.*, **11**, 95 (1931); **13**, 260 (1931).
5. S. ROTHSCHILD, *Physik. Z.*, **35**, 557 (1934).
6. J. EWLES, *Proc. Roy. Soc., London (A)* **167**, 34 (1938); *Trans. Faraday Soc.*, **35**, 124 (1939).
7. LECOQ DE BOISBAUDRAN, *C. R. Paris*, **103**, 1107 (1886).
8. E. IWASE, *Sci. Papers Inst. Phys. Chem. Research Tokyo*, **34**, 761 (1938).
9. KLEMENT, *Compt. rend. acad. sci. U.R.S.S.*, **46**, 270 (1945).
10. *C. A.* **35**, 7887 (1941).
11. German Pat. 711,437.
12. ALFRED H. MCKEAG AND PETER W. RANBY (To General Electric Co. Ltd., London) British Pat. 526,675, Sept. 24, 1940.
13. ROBERT C. PIERCE, U. S. Pat. 2,257,649, Sept. 30, 1941; TED E. FOULKE, U. S. Pat. 2,203,682, June 11, 1940, and U. S. Pat. 2,232,780, Feb. 25, 1941.
14. LECOQ DE BOISBAUDRAN, *C.R. Paris*, **103**, 629 (1886).
15. I. G. Farbenindustrie, A-G, British Pat. 460,210, Jan. 22, 1937.
16. G. TROEMEL AND H. MOELLER, *Z. anorg. u. allgem. Chem.*, **206**, 227 (1936).
17. W. F. BALE, J. F. BONNER AND H. C. HODGE, *Ind. Eng. Chem., Anal. Ed.*, **17**, 491 (1945).
18. F. A. KROEGER, "Some Aspects of the Luminescence of Solids," p. 183, (1948).
19. TH. P. J. BOTDEN AND F. A. KROEGER, *Physica*, **13**, 216 (1947).
20. L. THORINGTON, "Preparation and Characteristics of Luminescent Materials," p. 269, Cornell Symposium (1947).

SOME EFFECTS OF HEATING ZIRCONIUM IN AIR, OXYGEN, AND NITROGEN[1,2]

E. T. HAYES AND A. H. ROBERSON

Bureau of Mines, U. S. Department of the Interior, Albany, Oregon

ABSTRACT

Zirconium metal was heated in nitrogen, oxygen, and air at temperatures ranging from 425 to 1300 C. Observations were made on the gain in weight, micro- and macrohardness, and metallographic structures. Nitrogen diffuses into zirconium at a much slower rate than oxygen. A marked increase in penetration of both gases was found near 900 C, and this is evidently associated with the allotropic transformation from hexagonal, to cubic form. Practical limits for the heating of zirconium in air, oxygen and nitrogen are given and the possibilities of producing hard surface coatings are discussed.

INTRODUCTION

The advent of zirconium metal in quantities sufficient for thorough studies of the properties of the metal has been reported previously by the Bureau of Mines, U. S. Department of the Interior (1, 2, 3). This metal, which is produced by the magnesium reduction of zirconium chloride, continues to be the subject of considerable research. In the production of sheet, rod, and other shapes for various test purposes, it has been found (4) that the metal work hardens rather rapidly at room temperature and in general will take only 40 to 50 per cent reduction by cold working. The obvious answer of hot working is complicated by the fact that zirconium, when heated, reacts avidly with oxygen and nitrogen. It has been known for many years that small amounts of oxygen and nitrogen, when dissolved in the metal, cause it to lose its ductility, but no systematic approach seems to have been made to determine the effects of oxygen and nitrogen on ductile zirconium, that is, the limits to which it may be heated in either gas or air without impairing its desirable physical properties.

The investigation described in this paper was undertaken with the object of determining the practical limits to which Bureau of Mines zirconium could be heated in oxygen, nitrogen, or air without deleterious effects. As a secondary feature, the general nature and hardness of the surface coatings produced were studied from the standpoint of hard-surfacing materials for zirconium. The hardness of some of the films proved so interesting that attempts were made to determine their stability when reheated in air.

Fast (5) annealed zirconium made by the iodide process in vacuum, air, and a gas flame. His work was largely qualitative, in that it was restricted to a few minutes. He concluded that heating 3 to 5 minutes in air at 650 C was the maximum for thin (0.012 in.–0.305 mm) sheet.

[1] Manuscript received January 31, 1949. This paper prepared for delivery before the Philadelphia Meeting, May 4 to 7, 1949.

[2] Not subject to copyright.

De Boer and Fast (6, 7) also reported the influence of oxygen and nitrogen on the alpha to beta transition point and the electrolysis of solid solutions of oxygen in zirconium. In both cases, they were concerned with solid solutions and heated wire to 1900 K to dissolve the gas in the metal. Lilliendahl (8) and co-workers used somewhat the same method in investigating additions of oxygen to zirconium.

Hickman and Gulbransen (9) studied the oxidation films on zirconium and found that the solid metal disintegrated near 650 C.

Guldner and Wooten (10) worked on the reactions occurring when zirconium powder is exposed to a number of gases. Their primary interest was in the use of zirconium as a getter material, and since the work was done at low pressures on large specific surface areas, it was not applicable to the problem of heating massive zirconium in air.

It is apparent from all this work that oxide and nitride films can be formed at relatively low temperatures, and that solid solutions may be obtained by heating at temperatures high enough to promote diffusion. The medium range of temperatures, which are of interest in hot-working and annealing zirconium metal, have not been fully explored to explain when the internal diffusion of these gases into the lattice takes place. It should be possible to heat zirconium short of this point of permanent, irreversible hardening to facilitate working of the metal and still produce a satisfactory surface with the aid of mechanical or chemical cleaning.

EXPERIMENTAL PROCEDURE

Essentially, the experimental data were obtained by heating zirconium sheet in oxygen, nitrogen, and air for known periods at carefully controlled temperatures, and recording gain in weight and macro- and microhardness. All specimens were examined metallographically, and occasional x-ray analyses were made.

The zirconium sheet stock was produced from Bureau of Mines zirconium in which the principal impurities were iron, 0.05 per cent; carbon, 0.12 per cent; and oxygen, indeterminate, but believed to be less than 0.10 per cent. An ingot, protected from oxidation by an iron sheath, was forged and hot-rolled at 850 C to about 0.1 in. (2.5 mm) thickness. After the sheath was removed, the sheet was cleaned mechanically and cold-rolled 20 or 30 per cent to produce the 0.063 in. (1.6 mm) sheet stock employed for these tests. Cold-worked sheet was used because it is representative of the conditions that would be encountered in actual practice. Specimens were prepared by cutting the stock into sections about 0.75 x 1.5 x 0.063 in. (18.7 x 38 x 1.6 mm), cleaning in soap solution and carbon tetrachloride, rinsing in alcohol, and drying in warm air. Each specimen was measured, weighed, and numbered.

Individual specimens were placed in quartz tubes and backed up by a ball of zirconium shavings, so placed in the tube that it never attained the temperature of the specimen itself, but was still heated hot enough to act as a getter for water vapor, and in the nitrogen series to remove any residual oxygen. The efficiency of this protection in removing oxygen and water vapor was well illustrated in the experiments involving nitrogen. Simple sweeping of the tube with nitrogen, or evacuating and back-filling with nitrogen, did not produce an atmosphere of sufficient purity, since the

specimens turned bluish-black. Introduction of zirconium turnings produced golden-yellow surface films when the tube was evacuated and back-filled three times with nitrogen. A positive pressure inside the tubes was obtained by connecting a 12-inch rubber balloon filled with the desired gas directly to the quartz tube, thus insuring a slight pressure of the gas at all times.

The quartz tubes containing the specimens were inserted in tube furnaces and heated at the desired temperatures. After the heating period the tubes were withdrawn from the furnaces, cooled in air, and the specimens removed.

Heat resistance in air was determined in a muffle furnace, with the specimens maintained in a vertical position by being placed in slotted alundum plates. Holes in the door and the rear of the furnace furnished a slight air circulation and prevented the improverishment of oxygen in the furnace atmosphere during the run.

EXPERIMENTAL RESULTS

Air.—Changes in weight and hardness when Bureau of Mines zirconium is heated in air are presented in Table I.

The coatings are bluish-black and tightly adherent up to 600 C. White spots of zirconium oxide and accompanying flakiness appear at this point and increase steadily until the specimen is almost white after 24 hours at 700 C, 4 hours at 800 C, or a few minutes at 900 C. Specimens heated at 800 C and 900 C are an off-white with a yellow cast, although x-ray and chemical analyses failed to show the presence of ZrN.

It can be seen from the data plotted in Fig. 1 that there is a continued weight gain with increasing time and temperature. Up to 600 C, this gain in weight follows the equation of linear growth and probably holds true for the lower time periods at 700 and 800 C, but does not hold for 24-hour periods at these higher temperatures. In all probability, spalling of the oxide presents a fresh metal surface and thus increases the total gain in weight. Although the diffusion rate of oxygen through the ZrO_2—Zr interface is not known, it is reasonable to assume that an adherent oxide layer would act as an efficient barrier to retard the diffusion of the gas into the metal.

Microscopic examination of all specimens shows that there is no evidence of oxygen or nitrogen penetration into the body of the metal below 700 C. Short time exposures of less than one hour at 800 C produced only oxide surface layers and showed no evidences of further penetration. The specimens exposed for one hour and longer showed the intragranular rods and coarsened grain boundaries found in the oxygen series. In the 900 C series, it was found that the diffusion was extremely rapid. In one test with a thicker section, oxides were observed at the center of a quarter-inch (6.3 mm) sheet which had been held at this temperature only 30 minutes. It appears probable that this sudden vulnerability to oxygen penetration can be ascribed to the change in volume that takes place at 862 C when the close-packed, hexagonal, alpha phase transforms to the body-centered, cubic beta form. The two per cent volume change and the attendant shifting of atoms certainly afford ample opportunity for intergranular oxide formation.

Several minutes exposure to air at 800 C might be tolerated in certain cases where machining or deep-grinding operations would subsequently be

used as a final finish. On the basis of both gain in weight and metallographic evidence, zirconium cannot be heated for long periods at 800 C or any appreciable time at 900 C without losing its malleability.

TABLE I. *Gain in weight and hardness of zirconium metal heated in air*

Temperature C	Gain, mg/sq dm			Hardness, Rockwell B			Hardness, Knoop		
	1 Hour	4 Hours	24 Hours	1 Hour	4 Hours	24 Hours	1 Hour	4 Hours	24 Hours
425	7.6	11.4	36	88	88	87	227	224	227
500	36	63	159	81	81	80	296	298	352
*									
600	95	179	740	80	81	79	278	374	—
700	169	286	3,515	81	70	80**	486	—	—
800	326	565	5,930	80	—	—	—	—	—
900	6,500	—	—	—	—	—	—	—	—
Dry Air									
500	35			B 83			363		
600	63			84			232		
700	160			83			525		
*									
800	287			86			900		
900	2,170			—			—		

* This line indicates recommended heating limits.
— Indeterminate because of heavy oxide.
** Base metal after flaking off oxide.

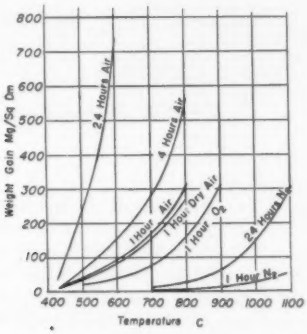

FIG. 1. Weight gain in Bureau of Mines zirconium heated in oxygen, nitrogen, and air.

Rockwell and Knoop hardness values must be accepted only as indications, since the character and thickness of the oxide coat influences both measurements.

Probably the most pronounced effect of heating zirconium to 900 C in moist air for an hour was the 15 to 18 per cent increase in dimensions. This was a marked variation from similar specimens heated at the same tempera-

tures in dry nitrogen and oxygen, which showed no perceptible change in size. This comparison is clearly illustrated in Fig. 2, where the entire suite of specimens which were heated for one hour is shown.

Dry air.—Check runs in dry air were made to determine the effect of humidity and these results are recorded in Table I. At the time these tests were made, the relative humidity ranged from 20 to 30 per cent. However, in some localities this figure often reaches 80 per cent during some seasons, so a comparison of results obtained here may be difficult to reproduce under other atmospheric conditions.

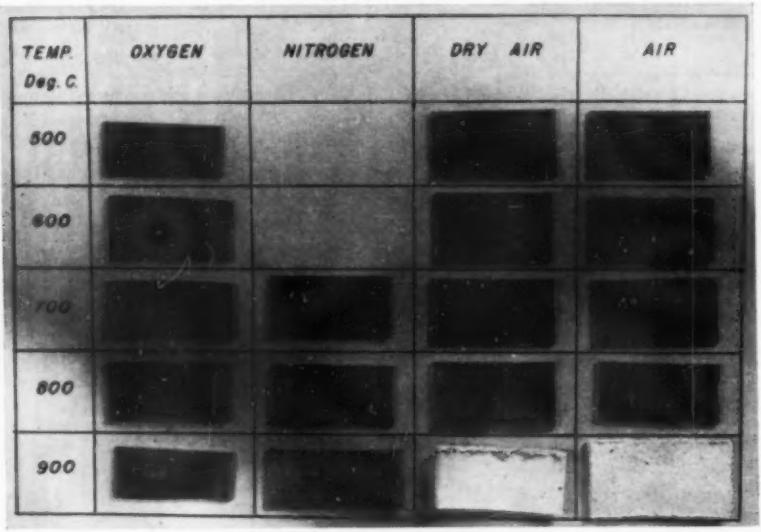

Fig. 2. Appearance of specimens heated for one hour in various gases

It is not immediately apparent from the weight gains that a humidity of this level plays a major role, since no marked differences were encountered. The hardness readings, however, show that the outer surface is consistently harder and reaches Knoop 900 at 800 C. This surprising development indicates that water vapor has a strong effect on the character of the surface coating, and may account for the excessive spalling found in zirconium heated at 800 and 900 C in air.

Dimensional growth of the 900 C specimen in this group amounted to 8 or 10 per cent, or approximately half of the increase recorded for the companion piece heated in moist air. Pronounced buckling of the specimen heated in dry air also was noted. This was the only specimen in the entire group which showed any distortion, an indication that from this one aspect, it may not have been truly representative.

Nitrogen.—Table II shows weight gain and hardness of zirconium after exposure to dry nitrogen.

The yellow nitride film produced at 700 and 800 C is so thin that the surface finish of the cold-rolled sheet is still evident. As this film thickens at higher temperatures, it deepens to an even golden color. This color is distinctive, the appearance of blue-black discolorations, or even a deep bronze color, indicates that the surface has been contaminated by oxygen.

The weight-gain data shown in Table II are plotted in Fig. 1. Heating one hour in nitrogen produces a small but almost linear increase over the range of temperatures studied. The longer heating time produces a more rapid absorption of nitrogen above 800 C.

Metallographic study shows that the nitride case formed at the lower temperatures is thin and adherent. No evidence of nitride penetration was observed in specimens heated at less than 1000 C. The first manifestation of penetration was a coarsening of the grain boundaries at the metal-case

TABLE II. *Gain in weight and hardness of zirconium metal heated in nitrogen*

Temperature C	Gain, mg/sq dm		Hardness, Rockwell		Hardness, Knoop	
	1 Hour	24 Hours	1 Hour	24 Hours	1 Hour	24 Hours
700	4.7	16	B 86	B 92	246	494
800	7.2	28	88	94	379	940
900	15	65	85	100	698	842
1000	27	140	83	C 19	502	829
1100	65	304	86	22	486	698
1200	102	572	89	23	736	736

* This line indicates recommended heating limits.

interface. At 1100 C the penetration was plainly evident, extending completely through the 0.063 in. (1.6 mm) specimen held at temperature for 24 hours. Heating for one hour at 1200 C likewise resulted in similar penetration by nitrogen.

The normal structure of annealed zirconium shown in Fig. 3 contrasts sharply with the widened grain boundaries of the specimen heated in nitrogen at 1200 C and shown in Fig. 4. Fig. 5 shows the penetration of the nitride case into metal, which was heated at 1200 C for 47 hours. The thin, dark needles appearing in the surface layer are typical of all thick nitride films. The appearance of rounded nitride areas within adjacent grains and marked grain-boundary widening also are shown.

X-ray analyses of wedges prepared from the center of the specimens failed to show the presence of ZrN or an expanded lattice up to 1200 C. Considerable difficulty was encountered in analyzing the case formed at 1000 and 1100 C by heating 24 hours, but there were indications of lattice expansion. The case formed at 1200 C showed a body-centered cubic pattern with an "a" value of 4.55 Å. A second phase near the bottom of the case is an expanded alpha zirconium lattice with an axial ratio of 1.599 compared to a normal c/a value of 1.588 listed by Barrett (11) and shows that some nitrogen is being retained in the alpha lattice.

Rockwell hardness readings follow a normal annealing schedule for the one hour exposure times up to 1000 C and then rise as the thickness of the nitride case increases. Heating 24 hours produces a definite hardening

effect even at 700 C. Knoop hardness readings are erratic at high temperatures where the ZrN coating shows cracking on a micro scale. Nevertheless, they indicate that a surface hardness near Knoop 900 can be produced by heating zirconium metal in dry elemental nitrogen.

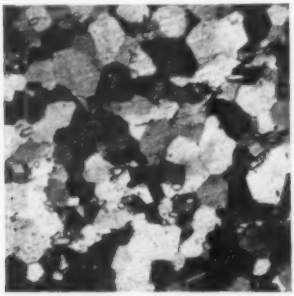

FIG. 3

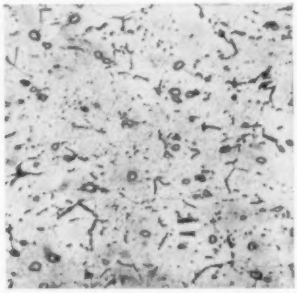

FIG. 4

FIG. 3. Appearance of annealed Bureau of Mines zirconium metal. Etchant, Vilella's reagent. × 125.

FIG. 4. Area near center of specimen heated in dry nitrogen for one hour at 1200 C. Etchant, Vilella's reagent. × 125.

TABLE III. *Gain in weight and hardness of zirconium heated in oxygen*

Temperature C	Gain in weight mg/sq dm	Hardness	
		Rockwell	Knoop
500	19	B 90	279
600	38	85	279
700	75	87	323
800	222	89	668
900	310	92	882

* This line indicates recommended heating limits.

Oxygen.—Zirconium was heated for one hour in dry oxygen at temperatures ranging from 500 to 900 C. The accompanying changes in weight and hardness are presented in Table III.

All specimens were blue-black and showed only traces of white oxide as compared to the metal heated in air. The coat was tightly adherent, as shown by the higher hardness level for both micro- and macrohardness values. The surface hardness of Knoop 882 is of the same order of magnitude as that produced by nitrogen or dry air.

Metallographic examination of these oxygen-treated specimens shows that there is no evidence of oxygen diffusing into the body of the metal until a temperature of 800 C is reached. The beginning of this diffusion is characterized by the appearance of small, rod-like markings in the grains near the surface of the specimen. At 900 C, Fig. 6, a bright, solid solution zone near the surface overlays an area in which the oxide occurs in the grain boundaries as well as within the grains.

Numerous difficulties were encountered where specimens were heated in oxygen at 1000 C, largely because of spontaneous ignition; as a result, no data are presented for this temperature. Its unpredictable behavior suggests that the ignition temperature of the solid metal in dry oxygen is slightly below 1000 C, since several of the specimens ignited and burned during these tests. Powdered zirconium, of course, behaves quite differently and ignites near 200 C.

Stability of oxide and nitride coats in air.—The possibility that the surfaces of specimens heated in oxygen or nitrogen might be rendered more resistant to atmospheric oxidation was investigated by reheating a few selected specimens in air (near 30 per cent humidity). A sheet had been heated previously in dry oxygen at 800 C for one hour; when reheated in air at 500 C, it showed very little weight change after four hours. After

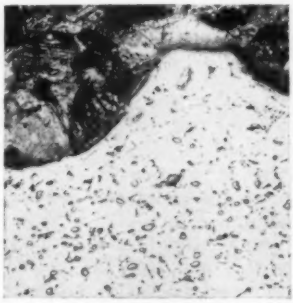

FIG. 5

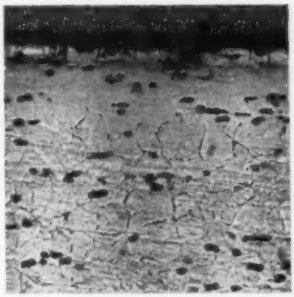

FIG. 6

FIG. 5. Nitride surface on zirconium heated at 1200 C for 47 hours in dry nitrogen. Etchant, Vilella's reagent. × 75.

FIG. 6. Oxygen penetration in zirconium heated for one hour at 900 C in dry oxygen. Etchant, Vilella's reagent. ×125.

seven hours at 600 C, a similar specimen showed a weight gain of 56 mg/sq dm with very little change in surface appearance.

Another specimen previously heated at 1100 C in dry nitrogen was likewise reheated at 600 C in air. After a short time at temperature, the nitride case broke away from the specimen in the form of a coherent brittle scale. Heating for 4 hours completely oxidized this scale to a voluminous grayish-yellow powder. At the same time, the surface of the specimen became covered with a continuous layer of white oxide similar in appearance to the coatings produced on specimens heated in air at 900 C. There is no doubt that the nitride surfaces are far more susceptible to attack than the oxide surfaces when heated in air.

DISCUSSION

These investigations were made to determine the practical limits to which Bureau of Mines zirconium could be heated in air and, as a secondary feature, to produce hard surface coatings. The data are not extensive enough to ascertain the diffusion rates of oxygen and nitrogen in the metal or to present equations expressing the amount of oxygen or nitrogen that

will be absorbed under a given set of conditions. It is realized that the data presented have certain limitations because only one type of zirconium metal was used, the surface finish represented only one specific set of conditions, and grain size was not controlled. Nevertheless, a number of generalizations can be made relating to the behavior of zirconium heated in air, oxygen, and nitrogen.

Gain in weight data can best be judged on the basis of figures set up for heat resistance. In such work a loss of 0.1 in. (.25 mm) of metal per year is one of the standards. Calculations for zirconium show that this amounts to a metal loss of about 450 mg/sq dm/24 hr, or, in terms of the data plotted in Fig. 2, a weight gain of near 600 mg/sq dm/24 hr for ZrO_2. It is on this basis and on metallographic evidence that the heavy lines have been drawn in Tables I, II, and III to represent safe heating limits. Heating in air and nitrogen for a few minutes at 800 C might be permissible in some instances. In practice, the choice of time, temperature, and atmosphere will have to be judged on such details as end use of fabricated or annealed product, thickness of stock, allowable loss of metal, and type of finish desired.

Metallographic examination places a limit of 800 C on dry oxygen atmosphere heat treatments, 900 to 1000 C for dry nitrogen, and 800 to 900 C in normal air for any appreciable time. Although gain-in-weight and hardness figures are not very conclusive, it is apparent that the allotropic transformation of alpha to beta zirconium definitely increases the diffusion of oxygen and nitrogen into zirconium. The alpha, or hexagonal, close-packed form changes into beta, a body-centered, cubic type, above 862 C, and the shift of atoms necessary to effect this change, coupled with a 2 per cent difference in density, makes the metal vulnerable to attack by both gases. There is no easy way of differentiating between the diffusion rates in alpha and beta zirconium and the added mobility due to increase in temperature. The presence of a dark, grain-boundary constituent in specimens cooled through the transformation temperature suggests that both gases are much more soluble in the beta form.

The results point to some interesting possibilities for producing hard surface coating on zirconium. Surface hardness values of Knoop 900 (near Rockwell C 65) can be attained by heating in dry air, oxygen, or nitrogen. The nitride coat is somewhat brittle and would be restricted to use in air at temperatures below 400–500 C. The oxide surface retains its hardness without flaking for a few hours' exposure at 600 C in air. Although surface films of high hardness can be formed by heating 24 hours at 1200 C in dry nitrogen, 1 hour at 800 C in oxygen or dry air, they would have limited use. The nitride samples would have to be heated to at least 1300 C in high vacuum to produce a tighter bond. Difficulties connected with obtaining high vacuum at such a temperature, the micro-cracking observed on the surface, and embrittlement due to intergranular penetration make the use of nitride surfaces questionable. It would appear that the hard oxide coats formed by heating in dry air or oxygen have better bonding and stability in air, as well as grain size control, and potentially have a much wider application.

Qualitative observations on the character of the oxide formed by heating nitride surfaces in air and the effect of limited amounts of water vapor have shown that both play a role in producing voluminous deposits at high

temperatures. The nature of the decomposition products formed when ZrN is heated in air indicates that nitrogen has more effect than 30 per cent humidity in producing spalling. Zirconium when heated in air evidently undergoes simultaneous attack by both oxygen and nitrogen. The nitride, being unstable in the presence of oxygen, decomposes to a voluminous oxide. For this reason, it is not recommended that zirconium be hot worked in air after annealing in nitrogen.

Extreme dimensional growth of zirconium heated one hour at 900 C in air explains the behavior of zirconium when worked near this temperature. Fine surface cracks which are produced by rupturing the hard surface became filled with oxide from both primary and secondary oxidation reactions. These points act as wedges and, combined with intergranular attack, result in complete breakdown of the metal.

SUMMARY

Zirconium prepared by the Bureau of Mines was heated in air, nitrogen, and oxygen. Permissible times of heating at various temperatures are set forth based on a weight gain of 600 mg/sq dm and metallographic evidence of penetration of oxygen or nitrogen into the metal.

Absorption of nitrogen by zirconium takes place at a much slower rate than absorption of oxygen.

At 900 C there is definite penetration of oxygen into the body of the metal (above 1000 C for nitrogen); this is probably associated with the allotropic transformation that takes place at 862 C.

Dense zirconium may be heated to almost 1000 C in dry oxygen without burning.

Surface hardness values near Knoop 900 (Rockwell C 65) can be attained by heating in dry air, oxygen, or nitrogen at appropriate temperatures. The oxide surfaces may have possible use, but definite restrictions are placed on the nitride coat due to breakdown when heated in air. The voluminous nature of the oxide formed by decomposition of the nitride in air suggests that the mechanism of corrosion in air at higher temperatures involves nitrogen as well as oxygen.

ACKNOWLEDGMENTS

The authors wish to express their appreciation to Dr. W. J. Kroll for his encouragement and assistance, to D. M. Mortimore for x-ray analyses, and to W. L. O'Brien and R. H. Robertson for performing many of the general measurements.

Any discussion of this paper will appear in the discussion section of Volume 96 of the TRANSACTIONS of the Society.

REFERENCES

1. W. J. KROLL, A. W. SCHLECHTEN, AND L. A. YERKES, *Trans. Electrochem. Soc.*, **89**, 263–275 (1946).
2. W. J. KROLL, A. W. SCHLECHTEN, W. R. CARMODY, L. A. YERKES, H. P. HOLMES, AND H. L. GILBERT, *Trans. Electrochem. Soc.*, **92**, 99 (1947).
3. W. J. KROLL, C. T. ANDERSON, H. P. HOLMES, L. A. YERKES, AND H. L. GILBERT, *J. Electrochem. Soc.*, **94**, 1–20 (1948).
4. Unpublished work of the Albany Station, Bureau of Mines.
5. J. D. FAST, *Metallwirtschaft*, **17**, 459–462 (1938).
6. J. H. DE BOER AND J. D. FAST, *Rec. trav. chim.*, **55**, 459–467 (1936).
7. J. H. DE BOER AND J. D. FAST, *Rec. trav. chim.*, **59**, 161–167 (1940).
8. W. C. LILLIENDAHL, D. M. WROUGHTON, AND E. D. GREGORY, *J. Electrochem. Soc.*, **93**, 235–247 (1948).
9. J. W. HICKMAN AND E. A. GULBRANSEN, *Anal. Chemi.*, **20**, 158–165 (1948).
10. W. G. GULDNER AND L. A. WOOTEN, *J. Electrochem. Soc.*, **93**, 223–235 (1948).
11. C. S. BARRETT, "The Structure of Metals and Alloys," McGraw-Hill Book Co., Inc., New York (1943).

THE RARE EARTH INDUSTRY[1]

HOWARD E. KREMERS

Lindsay Light & Chemical Company, West Chicago, Illinois

ABSTRACT

The industrial extraction of cerium and other rare earths from monazite sand is reviewed briefly, and the principal uses of the rare earths are discussed.

THE RARE EARTHS

The rare earths consist of the fourteen elements, lanthanum, cerium, praseodymium, neodymium, samarium, europium, gadolinium, terbium, dysprosium, holmium, erbium, thulium, ytterbium, lutecium, and element 61 (see Tacle I).

Three divisions of the rare earths are arbitrarily recognized, namely, the "cerium earths" consisting of the elements lanthanum to samarium, the "terbium earths" consisting of the elements europium to dysprosium, and the "yttrium earths" consisting of the elements holmium to lutecium with yttrium. Although yttrium is not a rare earth, it is always found in nature with the rare earths of higher atomic number, and its chemical properties are similar to those of the higher rare earths. There are no sharp distinctions between the three groups of rare earths since there is considerable overlapping in properties. The cerium earths are the most abundant and are of the greatest importance.

The rare earths are basic elements; the basicity of the trivalent rare earths decreases with increase in atomic number. Yttrium has a basicity comparable to that of the yttrium earths. Cerium (IV) is less basic than the trivalent rare earths (1). Precipitation pH values for the trivalent rare earths very from 6.32 to 8.23, and for cerium IV the value is pH 2.7.

The most important soluble salts of the rare earths are the nitrates, double nitrates with alkali metal nitrates, sulfates, and chlorides. Insoluble salts are the oxalates, fluorides, hydroxides, basic salts, and phosphates. The sulfates are less soluble in hot solution than in cold solutions. The double alkali sulfates of the cerium earths are insoluble, while those of the yttrium earths are soluble.

MONAZITE SAND

The only important ore of the rare earths is monazite sand, a cerium earth orthophosphate containing thorium. Monazite occurs as brown monoclinic crystals having a hardness of 5–5.5 (Mohs's scale) and a specific gravity of 5.0–5.5. Small crystals of monazite occur in many granites and pegmatized gneisses, the amount rarely exceeding 0.1 per cent, and larger crystals occur in some pegmatites. Massive monazite is rare. Monazite sands are concentrated in stream and beach placers and in dunes in many parts of the world. The monazite sand in such placers occurs in small

[1] Manuscript received January 4, 1949. This paper prepared for delivery before the Philadelphia Meeting, May 4 to 7, 1949.

grains associated with other heavy mineral sands such as magnetite, ilmenite, rutile, zircon, and garnet. Monazite is separated from these sands by gravity and electromagnetic methods.

Most of the world's production of monazite has come from beach sands at Travancore, India, and from the states of Espirito Santo, Bahia, and Rio de Janeiro in Brazil (2, 3). Most of the monazite now consumed is produced in Brazil. Up to 1909, there was significant production of monazite from North and South Carolina. From 1909 to 1948, no significant amounts of monazite were produced in the United States. In 1948, monazite production was started in Florida and Idaho. World production of monazite sand for the past 50 years has averaged about 2,500–3,500 short tons annually.

TABLE I. *The rare earths and yttrium*

Element	Atomic number	Atomic weight	Valences	Oxide (ignited in air)	
Lanthanum	57	138.93	3	La_2O_3	Cerium group
Cerium	58	140.13	3, 4	CeO_2	
Praseodymium	59	140.92	3, 4	Pr_6O_{11}	
Neodymium	60	144.27	3	Nd_2O_3	
—	61	—	—	—	
Samarium	62	150.43	2, 3	Sm_2O_3	
Europium	63	152.0	2, 3	Eu_2O_3	Terbium group
Gadolinium	64	156.9	3	Gd_2O_3	
Terbium	65	159.2	3, 4	Tb_4O_7	
Dysprosium	66	162.46	3	Dy_2O_3	
Holmium	67	163.5	3	Ho_2O_3	Yttrium group
Erbium	68	167.2	3	Er_2O_3	
Thulium	69	169.4	3	Tm_2O_3	
Ytterbium	70	173.04	2, 3	Yb_2O_3	
Lutecium	71	174.99	3	Lu_2O_3	
Yttrium	39	88.92	3	Y_2O_3	

Prior to about 1920, monazite was sold on the basis of its thorium content, and rare earth chemicals were produced as by-products from the manufacture of thorium nitrate for incandescent gas mantles. Since 1920, monazite has been worked chiefly for cerium, and monazite is sold on the basis of its rare earth oxide content. Monazite and other thorium minerals are controlled by the Atomic Energy Commission; rare earth chemicals are exempted from control.

A typical refined monazite sand has the following approximate analysis: La_2O_3—15.6%; CeO_2—28.8%; Pr_6O_{11}—3.6%; Nd_2O_3—11.4%; Sm_2O_3—1.2%; terbium earth oxides—0.8%; yttrium earth oxides—0.32%; ThO_2—6.5%; U_3O_8—0.2%; CaO, Fe_2O_3, Al_2O_3, etc.—1.0%; SiO_2—1.5%; and P_2O_5—28%. In addition, monazite contains small amounts of radium and mesothorium. The 1948 world price for monazite sand containing a minimum of 60 per-centr are earth oxide or about 95 per cent monazite was $105 per metric ton.

INDUSTRIAL RARE EARTH CHEMICALS (4)

Commercial production of rare earth materials began in 1885 with the manufacture of thorium nitrate from monazite sand for use in incandescent

gas mantles. At that time, the rare earths were a by-product of the refining of thorium. With the development of uses for the rare earths, the demand for rare earth materials increased and thorium became a by-product of the rare earth industry, a situation which exists even today.

Treatment of monazite

The extraction of the rare earths from monazite involves three steps: opening the ore, separation of thorium, and isolation of the rare earths.

Monazite sand is converted to anhydrous rare earth sulfates and phosphoric acid by heating with sulfuric acid. A mixture of monazite sand and up to three times its weight of concentrated sulfuric acid is heated and stirred in cast iron pots until the reaction is complete. The cooled product is leached with water to dissolve the anhydrous rare earth sulfates. Thorium is removed by diluting the solution to precipitate selectively thorium phosphate, or the thorium may be precipitated with sodium pyrophosphate or with the addition of a base to precipitate basic thorium salts.

The rare earths remaining in the solution after precipitation of thorium are then isolated and freed of most of the phosphoric acid present by precipitation with alkali hydroxides, oxalic acid, or sodium sulfate. In the latter case, insoluble cerium earth double sulfates are precipitated, leaving a large proportion of the yttrium earths in solution.

The rare earth precipitate is recovered by filtration and may be converted to rare earth hydroxides by boiling with sodium hydroxide. Rare earth salts are made from these hydroxides by treatment with the appropriate acid.

Cerium separation

Cerium is separated from the other rare earths by oxidation to the ceric state (cerium IV), followed by precipitation of an insoluble ceric compound.

Cerous salts can be oxidized to ceric salts in acid solution with ammonium persulfate, bismuth tetroxide, lead peroxide, or by electrolysis. In basic slurries, cerium is oxidized by treatment with alkali hydrochlorites, permanganates, oxygen, and air. In these oxidations, the other trivalent rare earths are unaffected. Ceric salts are generally much less soluble than the corresponding cerous or trivalent rare earth salts. Cerium IV precipitates at pH 2.7 whereas trivalent rare earths are precipitated at pH 6 to 8 depending on the particular rare earth. Thus, basicity methods can be used for separating cerium IV from the rare earths. Many methods have been devised for the separation of cerium, but the following are the most important.

Starting with the crude rare earths obtained from monazite (containing about 50% cerium), one treatment by any of the cerium separation methods rarely gives cerium products containing less than 0.5 to 1 per cent of other rare earths. Repetitions of the process or changes to more suitable methods will give cerium materials containing insignificant amounts of other rare earths.

Crystallization of ammonium hexanitratocerate.—Ammonium hexanitratocerate, $(NH_4)_2[Ce(NO_3)_6]$, is slightly soluble in nitric acid solutions, whereas

the trivalent rare earth nitrates and double ammonium nitrates are soluble salts. To effect a cerium separation, the crude cerium material is converted to a ceric nitrate solution in nitric acid. This is easily accomplished by dissolving rare earth oxides or hydrated oxides in nitric acid; during the ignition of rare earth oxides, cerium III is completely oxidized to cerium IV. An excess of ammonium nitrate over that required to form $(NH_4)_2[Ce(NO_3)_6]$ is added to the hot solution, and the orange crystals of ammonium hexanitratocerate are removed by filtration after cooling. The cerium product usually is 99.5 per cent pure; additional crystallizations give cerium materials which are pure within the ordinary limitations of analytical accuracy.

Crystallization of ammonium trisulfatocerate.—Cerium is similarly crystallized from a sulfuric acid solution containing cerium IV by the addition of ammonium sulfate to crystallize $(NH_4)_2[Ce(SO_4)_3]\cdot 2H_2O$. This method of separation is not as efficient as the ammonium hexanitratocerate method.

The bromate and permanganate methods.—The classical bromate method (5, 6, 7) is applicable only to small scale operation. Potassium bromate is added to a hot neutral solution containing cerous nitrate, and cerium is oxidized and precipitated as a basic ceric salt. The solution is kept neutral by the addition of marble. In the permanganate method, alkali permanganate is added to a hot, neutral cerous salt solution, and the oxidized cerium is precipitated by phosphates (8) or alkalies (9).

Electrolytic oxidation of cerium.—Electrolytic oxidation of cerium in acid solutions followed by precipitation of insoluble cerium IV compounds will also separate cerium from the other rare earths since the latter are not affected by the electrolysis. In sulfate and nitrate solutions, anodic oxidation of cerium usually goes to 90 per cent completion, and the addition of a precipitant for cerium IV will give 99 per cent oxidation and precipitation of cerium (8). With sulfate and nitrate solutions, a diaphragm cell is not required because anions containing cerium IV are repelled from the cathode. Chloride solutions, however, require a diaphragm cell. Platinum or lead dioxide anodes are satisfactory, and the anode area must be considerably greater than the cathode area (10).

Precipitation of basic ceric salts.—When nitrate or sulfate solutions containing cerium IV are diluted with water, basic ceric salts are precipitated, while trivalent rare earths under the same conditions are not precipitated (11, 12). This method for separating cerium is efficient, especially when basic ceric nitrate is precipitated.

Partial dissolution of hydrated rare earth oxides.—When rare earth hydroxides containing cerous hydroxide are dried in air, the dried material consists of hydrated oxides containing hydrated ceric oxide. The partial dissolution of these hydrated oxides by acid will leave cerium IV in the insoluble residue if the pH of the system is maintained below that required for precipitation of trivalent rare earths and above that required for precipitation of cerium IV (12).

Separation of the rare earths

With few exceptions, the cerium-free rare earths are separated by complicated and tedious fractional crystallizations of soluble salts. Lan-

thanum is purified commercially by crystallization of its double ammonium nitrate, and neodymium is made by a similar procedure. Small amounts of samarium, europium, and gadolinium concentrates are made with laboratory-scale operations.

USES OF THE RARE EARTHS

Cerium is the most important rare earth commercially. It is often used in the form of mixed rare earth materials where the cerium is approximately 45–50 per cent of the rare earths. Commercial "rare earth" materials generally contain rare earths in the ratios in which they are found in monazite sand. Commercial cerium compounds usually contain up to 2 per cent other rare earths as impurities, and technical grades may contain considerable phosphate. Refined and reagent grade cerium compounds contain only traces of other rare earths.

Many of the uses of the rare earths are based on the characteristic absorption spectra of the rare earths. All of the rare earths except lanthanum and lutecium have sharp, narrow absorption bands in the visible or ultraviolet spectra. Cerium absorbs most strongly in the ultraviolet.

The principal uses of cerium and the rare earths are as follows:

Glass decolorization.—Cerium IV is an oxidizing agent and oxygen carrier in glass melts, oxidizing iron so that the glass is decolorized and is stable toward solarization and reheating. Manganese oxide or permanganates, didymium (cerium-free rare earths) carbonate, rare earth hydrate, cobalt oxide, and selenium may be used as physical decolorizers in combination with cerium.

Glass coloring.—With titanium, cerium imparts a yellow color to glass due to the formation of yellow cerium titanate. Neodymium is used for purple glass having a distinctive color not obtainable with other materials, and in the manufacture of certain ophthalmic lenses where absorption of yellow light is required. Glassblowers' goggles contain neodymium which almost completely absorbs the yellow sodium light.

Cerium compounds are opaque to ultraviolet light, and in glass they eliminate the transmission of ultraviolet light.

Glass polishing.—Specially prepared rare earth and cerium oxides are used for polishing optical glass and spectacle lenses. Cerium oxide polishes faster than rouge and is cleaner to use, and for these reasons is preferred by many polishers.

Optical glass.—Purified lanthanum oxide containing less than 0.01 per cent other rare earths is used in silica-free optical glass having a high index of refraction and low dispersion. This type of glass is used for components of camera lenses in higher-priced cameras, and in aerial photography lenses. Lanthanum oxide in optical glass increases the index of refraction.

Opacifiers.—Ceric oxide has been used in Europe as a mill addition opacifier in white vitreous enamels. A typical mill addition frit contains about 2 per cent CeO_2. Cerium oxide is used in this country as an opacifier in porcelain glazes where pastel colors are desired.

Rare earth metals and alloys.—About one-quarter of the rare earths produced commercially are eventually used in the metallic state or in alloys. Partially dehydrated rare earth chlorides are heated in iron pots to drive off the water of hydration, fluxing salts are added to the anhydrous

chlorides thereby formed, and heating is continued to produce a melt. The dehydration produces some rare earth basic chlorides which aid in keeping the melt fluid. The melt is then electrolyzed in the iron pot (cathode) with an iron or carbon anode. The molten metal collects on the bottom of the pot and is cast in steel molds under a layer of molten flux.

"Misch metal" or "mixed metal" is an alloy of cerium with the other rare earths. Commercial misch metal contains 45–50% Ce, 22–25% La, 15–17% Nd, and 8–10% other rare earth metals, up to 5% Fe, 0.1–0.3% Si, and traces of calcium, carbon, and aluminum.

Ferro-cerium, Auer metal, etc., are iron-cerium alloys containing 10–65 per cent iron, misch metal or cerium metal, and traces of other metals as impurities. Pyrophoric iron-cerium alloys for use as spark metal (lighter flints, etc.) contain 18–30 per cent iron, and small amounts of zinc, aluminum, magnesium, calcium, and silicon. Iron is necessary in spark metal to increase its hardness.

Carbon arcs.—Cerium group oxides and fluorides are used in the cores of flame arc carbons where a white light is desired. The light quality from such carbon arcs closely matches the color quality of natural sunlight; such lights are used for broadside lighting in motion picture studios (13).

Reagent chemicals.—Ammonium hexanitratocerate is typical of the cerium salts used as analytical oxidimetry reagents (10). A rare earth oxalate preparation is used medicinally to treat seasickness and prevent nausea.

CONCLUSION

The rare earths have been produced commercially on a relatively large scale for many years, and they are not as unavailable or as expensive as their name implies. Commercial rare earth materials vary in price from about 35 cents to several dollars per pound. As interest in the rare earths grows, more uses will be found for them, for they are a unique group of elements.

Any discussion of this paper will appear in the discussion section of Volume 96 of the TRANSACTIONS of the Society.

REFERENCES

1. T. MOELLER AND H. E. KREMERS, *Chem. Revs.*, **37**, 97 (1945).
2. A. V. PETAR, *U. S. Bur. Mines Inform. Circ.*, 6847 (1935).
3. L. G. HOUK, *ibid.*, 7233 (1935).
4. H. E. KREMERS, "Encyclopedia of Chemical Technology," Vol. **3**, Chapter on "Cerium," Interscience Publishers, Inc., New York (1949).
5. C. JAMES AND L. A. PRATT, *J. Am. Chem. Soc.*, **33**, 1326 (1911); **34**, 757 (1912).
6. H. F. V. LITTLE, "The Rare Earth Metals," in FRIEND, "A Text-Book of Inorganic Chemistry," Vol. **4**, pp. 320–321, 332–338, 384, Griffin, London (1921).
7. W. PRANDTL AND J. LÖSCH, *Z. anorg. allgem. Chem.*, **127**, 209 (1923).
8. J. W. NECKERS AND H. C. KREMERS, *J. Am. Chem. Soc.*, **50**, 950 (1928).
9. E. J. ROBERTS, *Am. J. Sci.*, **31**, 350 (1911).
10. G. F. SMITH, "Cerate Oxidimetry," G. F. Smith Chem. Co., Columbus, Ohio (1942).
11. L. WEISS (to Deutsche Gold und Silber Scheide-Anstalt) U. S. Pat. 2,222,924, Nov. 26, 1940.
12. J. BLUMENFELD, U. S. Pat. 2,327,992, Aug. 31, 1943.
13. W. C. KALB, "Encyclopedia of Chemical Technology," Vol. **2**, p. 905, Interscience Publishers, Inc., New York (1948).

MELTING AND CASTING ZIRCONIUM METAL[1, 2]

W. J. KROLL AND H. L. GILBERT

Northwest Electrodevelopment Laboratory, Bureau of Mines, Albany, Oregon

ABSTRACT

This report deals with the methods for melting and casting zirconium. Reference is made to the manner of heating, furnace design, crucible materials, and methods of casting. For the experiments, a high-frequency furnace, an arc furnace, and a split-tube graphite-resistor furnace were used. Preference is given the latter for vacuum fusion, while the high-frequency and the arc furnaces are well adapted for melting in a noble gas atmosphere. The crucible materials are discussed, and the melting in graphite and the casting of ingots are described.

GENERAL CONSIDERATIONS

The melting and casting of zirconium and titanium present many difficulties owing to their high melting point and chemical activity. These two factors restrict the means of heating, the furnace atmosphere, and especially the crucible and mold materials. Titanium will be mentioned only occasionally in this report because of its similarity to zirconium. The use of a nonreacting atmosphere, or of a vacuum, calls for construction that makes the crucible and mold difficultly accessible for tapping and pouring.

Crucible materials.—The crucible materials to be used may depend on the type of furnace. The only furnace not requiring a true crucible is the arc furnace, in which the metal may be fused on a water-cooled copper block. The fused cakes are small. A further development of this method consists of using a thin copper crucible which is intensively cooled to prevent alloying with the charge.

One of the authors has shown that all known refractory oxides react with zirconium and titanium (1, 2) or, in some instances, the refractory oxides dissolve as such in the metals. The equilibrium between such oxides and the metals may be shifted if the base metal of the oxide is more volatile than zirconium or titanium, as is the case with calcium oxide. This is particularly true in a vacuum as was noted by de Boer (7), who employed zirconium to produce calcium from its oxide. Later, the same reaction was described by Lilliendahl (10), who confirmed the previous work, so it is apparent that complete removal of oxygen from zirconium or titanium by use of calcium as a reducing agent cannot be accomplished. Pressure favors reduction of zirconium oxide to metal, but in a vacuum zirconium will reduce calcium oxide to calcium metal.

As has also been described in our previous work (1, 2), thoria is the best refractory oxide for melting titanium or zirconium. This has been re-examined subsequently and confirmed by Lilliendahl (10) and Brace (8). Small

[1] Manuscript received February 4, 1949. This paper prepared for delivery before the Philadelphia Meeting, May 4 to 7, 1949.

[2] Not subject to copyright.

amounts of thorium do not appreciably harden zirconium and titanium (1, 2). Highly fired thoria reacts only slightly with these metals, even at their melting point, but it is rather expensive and is now difficult to obtain, so may hardly be considered suitable for melting large quantities of zirconium and titanium.

Beryllia, which was used in early work (1, 2), is somewhat attacked, and beryllium hardens the metals. Very highly fired beryllia is less susceptible to attack but prohibitive in cost.

Zirconia crucibles are rapidly attacked by molten zirconium and titanium, which pick up oxygen or dissolve the oxide. Alumina behaves similarly (1, 2).

The discovery made at the Albany Station of the U. S. Bureau of Mines two years ago that titanium, zirconium, thorium, and probably hafnium may be melted satisfactorily in gas-free graphite (4, 5, 6) was of considerable importance, as it at once opened the road for melting large quantities of metal. It is particularly fortunate that a small amount of carbon is actually beneficial for many applications of these metals. We have found that zirconium, when melted in graphite, picks up between 0.15 and 0.25 per cent carbon; titanium, between 0.4 and 1.2 per cent; and thorium, between 0.1 and 0.2 per cent. If excessive temperature is employed for a long period, more carbon will be picked up, resulting ultimately in formation of the pure metal carbide.

The type of graphite used is important. Commercial electrode graphite is very porous and quite easily penetrated by the highly fluid molten metals which wet the graphite. We employ carefully machined crucibles of grade AUF or AUC graphite. The latter is quite gas free and may be used without degassing. Both grades are of special type, and are more expensive than electrode graphite.

No reduction of the oxide content of these metals is effected by melting in graphite. As reported some time ago by one of the authors (11) and confirmed by others (19), this reaction is quite commonly known to produce, even in vacuum, the so-called carboxides. Such carboxides may be used as refractories with some success, as they do not give off carbon monoxide at the temperature and pressure of vacuum melting. Some oxide contamination of the metal is found, however, owing to dissolution of the carboxide in the metal. No advantage of the carboxide refractories over plain graphite is apparent.

Carbides, borides, and some other high-melting compounds of zirconium and titanium have been considered. The borides have a very high melting point and are no more soluble in the fused metal than the carbides, but production of cheap, nonporous crucibles has proved to be a difficult problem.

Furnaces.—The vacuum arc furnace was introduced by von Bolton (12), who employed it with success in the fusion of tantalum. Moore (13) later proposed using the same type of glass-vessel furnace in melting thorium. Kroll (1) developed this furnace further by going to an all-metal shell, replacing the rubber joints with flexible metal tubing, and adding a tungsten tip to the electrode. Parke (14) made a further modification of this furnace for melting molybdenum, in which he employed compressed powder rods and a water-cooled copper mold.

Arc melting is no simple operation. In vacuum, the phenomena of gas

discharge and metal evaporation must be taken into consideration. Besides this, magnesium and magnesium chloride, which are present in the zirconium sponge in an amount usually not exceeding 0.1 per cent for both impurities combined, help initiating and maintaining the arc by the ionization of their vapor. The "sparking voltage," or that voltage at which the furnace atmosphere becomes sufficiently conducting to carry the discharge, depends upon many factors, of which the residual gas pressure must be considered foremost. In the presence of a residual gas, the sparking voltage reaches a minimum at a certain pressure, depending on the particular gas present (15). With a hot tungsten-wire cathode and with a tungsten-pin anode at a distance of 15 mm, the following minimum sparking voltages were observed: 75 volts, 0.6 mm Hg for hydrogen; 35 volts, 0.5 mm Hg for argon. It can happen that the residual gas might be more conducting than the metal vapor in the arc, causing a glow discharge to appear, after which little or no heat will go into the charge. This also shows that operation above the minimum gas pressure may be desirable to avoid the glow. A residual gas, if added deliberately, should have the highest possible sparking voltage. Hydrogen and helium are well suited for this use.

In addition to the sparking voltage, one must consider initiation of discharge. Thermionic emission is one cause. Certain metal oxides, especially calcium or barium oxide, condition the surface of the hot electrode to promote glow at low voltages. It is conversely true that many times when pressure conditions are highly favorable for glow, it will not appear if it is not initiated in some way. This shows why it is possible to operate furnaces with internal nichrome heating elements at 220 volts and 950 C through the entire critical range of pressure without glow appearing.

Striking an arc on a metal causes evaporation of the metal. Magnesium, which has a high vapor pressure, cannot be melted in vacuum, particularly by arc methods, because all the heat transferred would be dissipated by evaporation if under proper pressure conditions. Magnesium can be melted in vacuum if held under its own vapor pressure. If a large excess of energy is applied to magnesium in an evacuated but covered crucible, enough magnesium vapor is produced to force the fusion to take place. This is not truly fusion "in vacuum," as considerable pressure of metal vapor is present in the crucible room, the vacuum or the residual gas pressure being measured outside the crucible at the furnace shell.

Because of these considerations, vacuum arc melting in an open crucible is feasible only with metals having a comparatively low vapor pressure at their melting point, and special conditions must prevail in the crucible so that some metal vapor pressure can build up. Melting in a copper sleeve meets these requirements fairly well, since the vapor can pile up, bringing the temperature and pressure of the metal above the triple point. With titanium and zirconium, arc melting is possible, even on an open water-cooled copper plate, as mentioned above. Evaporation is noted, but does not reach excessive proportions.

Arc melting is easier under atmospheric pressure of an inert gas. Depending upon the type of furnace and the degree of cooling, the problem of expansion of this inert gas may be more or less important. In a small furnace employing a copper-sleeve-type crucible allowing thorough cooling, this phenomenon is not important; but with a larger furnace, as is des-

scribed later in this article, the furnace gas expands violently, and provision for relief must be made for safe operation.

The advantage of vacuum melting to remove hydrogen from zirconium and titanium is only partly found in operating under atmospheric pressure of an inert gas. Depending upon the volume of inert gas present, the degassing may be more or less successful, with the hydrogen dissolving in the noble gas, the hydride being in equilibrium with the dissolved hydrogen of the protective gas. At the melting point, both zirconium and titanium are virtually free of hydride, it being entirely dissociated even in an atmosphere of pure hydrogen. It is possible to melt these metals under a few centimeters pressure of hydrogen in the arc furnace on a water-cooled copper plug, since cooling is so rapid that back formation of hydride is negligible. Slow cooling in noble gas containing hydrogen, however, will lead to hydrogen pick-up.

Certain other impurities found in the zirconium or titanium powder or sponge, such as the chlorides of calcium and magnesium, are removed very well in vacuum fusion. Some lower chlorides of zirconium and titanium may also be present and will likewise be removed.

The removal of these impurities, especially magnesium chloride, is an advantage of fusion over powder metallurgy. The core of heavy sections of titanium made from magnesium-reduced metal by powder metallurgy after sintering always contains magnesium chloride and may show weakness in rolling.

A possible melting method for such powders would be by means of a tungsten-electrode radiation arc furnace, melting taking place on a pad of metal powder that would add no new impurities.

A definite advantage is gained in operating an arc furnace under atmospheric pressure in that it greatly simplifies the operation of the arc electrode. In vacuum, movable electrodes, if put through the furnace shell, require compensation against atmospheric pressure, for instance, by springs. This can be avoided by building the electrode control inside the furnace shell, as done by Parke (14), but this leads to a complicated internal mechanical construction which in time becomes contaminated with volatilized impurities (magnesium chloride) with subsequent evolution of gas during later runs.

Arc melting, in general, is limited by the maximum power input in the arc, the voltage for a zirconium and titanium arc being about 20–25 volts, which is not very high. A longer arc would result in higher voltage, as is employed in melting steel; in this case, however, a large part of the energy of the longer arc would be dissipated laterally to the water-cooled copper sleeve.

The question of electrodes for the arc furnace is also a matter of concern. The largest wrought-tungsten electrodes available in commerce are about $\frac{3}{4}$ inch (1.9 cm) in diameter. With most intensive cooling, these electrodes will carry an input of about 1,500 amperes, which will permit fusion of ingots up to perhaps 6 inches (15.2 cm) in diameter. For larger ingots, tungsten electrodes may have to be bundled.

We have suggested, as alternate electrode materials, zirconium and titanium carbide (3). Other carbides, such as tantalum carbide, might be quite as applicable. Such electrodes can be prepared by sintering compacts of the synthetic carbide and later impregnating them with molten

zirconium, titanium, or tantalum metal. They can be cast into or sweated to copper for cooling in operation.

Contamination of the ingot by the electrode material is small if the electrode remains clean. Should material from the molten bath spatter up onto the electrode, it will later, in a hot run, drip back into the bath, contaminating the melt. Neither carbon nor tungsten does much harm to titanium or zirconium, provided the contamination is small.

Feeding of the arc furnace with metal depends upon the form of the metal to be added. Powder is usually poured in, while sponge is briquetted and fed in that form.

High-frequency furnace.—The voltage across the coil of a high-frequency furnace is the most important item to consider when this method of melting in vacuum is used. The high-voltage, spark-gap, or R. F. type furnaces cannot operate with the coil in the furnace chamber because there will be discharge across the coil in vacuum. If the furnace embodies a quartz tube as the vacuum container with the coil outside this tube, satisfactory operation is assured, but there are limitations of size.

With the coils built into the vacuum chamber, it is generally accepted that a motor-generator set energizing the coil at less than 110 volts should be used. Such a set was employed by Heraeus (17) to melt steel. The steel-furnace shell must be shielded with a copper liner to prevent induction. Introduction of the furnace leads must be either concentric or so arranged that loss of energy by induction in the shell is minimized. All difficulties resulting from the volatilization of carbon in vacuum at high temperature and its subsequent reaction with hot silica walls must be dealt with.

Melting in a high-frequency furnace under atmospheric pressure of a noble gas does not offer any special difficulty, as will be shown later.

Carbon-resistor furnace.—This type was favored in our previous development because of its simplicity and efficiency (5). This furnace is essentially a radiation-type furnace in which a split-graphite tube resistor supplies the radiant energy. The limitations as to size depend upon the crucible only, since the resistor may be made of multiple plates as also shown by Poland (16). Horizontal arrangement of such plates leads to a trough-type furnace, which may offer advantages if the metal is to be poured over the rim into a mold. Such a horizontal, tiltable, heat-radiation furnace is being considered.

Casting zirconium and titanium.—The only possible methods for casting are by tapping or pouring over the rim.

In arc-furnace melting, employing a water-cooled copper sleeve, the ingot is built up progressively and not tapped. Such ingots have no pipe but often have surface imperfections and cold shuts, which require some machine work to remove them. Theoretically, any size of ingot may be built up in this way.

Arc melting, with formation of a pool, in view of tapping or pouring, is possible but necessitates the use of graphite as crucible material. Such furnaces are difficult to build, particularly for vacuum melting.

High-frequency melting and casting are comparatively easy if the operation is carried out in an inert gas as described by Rohn (18). The tap hole in a graphite crucible is closed with a plug of solid metal, which is melted out by a small, high-frequency coil when pouring is desired. Rohn also employed a tilting, low-frequency furnace for pouring over the rim. Ingot

casting in a graphite-resistor furnace is easy when using the plug method described below.

EXPERIMENTAL WORK

The arc furnace, high-frequency furnace, and several split-tube graphite-resistor furnaces were employed for melting and casting zirconium. Each of these types has advantages and disadvantages, and many different requirements are met in their work. No definite conclusion is made regarding the choice of one type over the others.

The factors influencing the choice of a furnace are as follows: the permissible contamination, the size and shape of the ingot, the cost of the melting operation, and the cost of the equipment involved.

The direct-current arc furnace which we use is an enlarged modification of one previously described (1). Construction is shown in Fig. 1. The water-cooled, tungsten-tipped electrode can be moved in any direction, both horizontally and vertically, by means of the flexible metal tubing by which it is introduced. The somewhat violent expansion and contraction of the inert atmosphere, when striking the arc, are taken care of with the automobile-tire inner tube attached. A funnel of molybdenum sheet delivers compressed zirconium briquets from a side-arm feeding device to the thin graphite crucible. This crucible is thermally insulated from the water-cooled copper-anode block by graphite radiation baffles, and the whole assembly is packed in tungsten wool to prevent radiation laterally to the furnace shell. With an input of 600–800 amperes, it is possible to melt 5 pounds of metal in about 3 minutes. Usual ingots are well fused and homogeneous and contain only a trace of tungsten and 0.02 to 0.07 per cent carbon. The carbon pick-up is small because of the rapid fusion. There is no question that this furnace could easily be improved to produce large ingots with low carbon and tungsten contamination. It may be possible to use alternating current in arc melting, but tungsten contamination may be expected to increase. Direct current, with the tungsten tip cathodic, permits a lower temperature of the upper electrode, but direct current is more expensive to produce. The 20–25 volts employed in melting zirconium in the arc furnace is not much higher than the 17 volts now employed in the graphite-resistor furnace, but the much higher rate of fusion in the arc furnace indicates a higher efficiency by this method.

High-frequency melting.—A very simple method of melting in a high-frequency furnace is shown in Fig. 2. A graphite crucible is placed in an ordinary high-frequency furnace and packed with lampblack for insulation. A tightly-fitting cover and graphite plumbing maintain a slight flow of pure helium or argon into the crucible. The charge of 16 to 20 pounds of zirconium is melted in about 20 minutes with an input of less than 40 kw after which it is allowed to cool in the crucible. While this method involves loss of a crucible for each melt, it makes possible easy melting of zirconium and titanium in any commercial high-frequency furnace.

Casting ingots by this method requires bottom tapping by use of an auxiliary high-frequency coil, a resistance heater, or an arc "stinger." As the mold also has to be purged with helium, the high-frequency coil, crucible, and mold must be placed inside a steel shell where the atmosphere can be closely controlled. A furnace of this type is under construction.

Split-tube carbon-resistor furnace.—This very successful and cheap method

of melting is used for all zirconium produced at the Albany, Oregon, station. The single-phase split-tube graphite-resistor furnace has been described previously (4). A three-phase model of this furnace has been found quite successful and offers several advantages. Most important of these are the

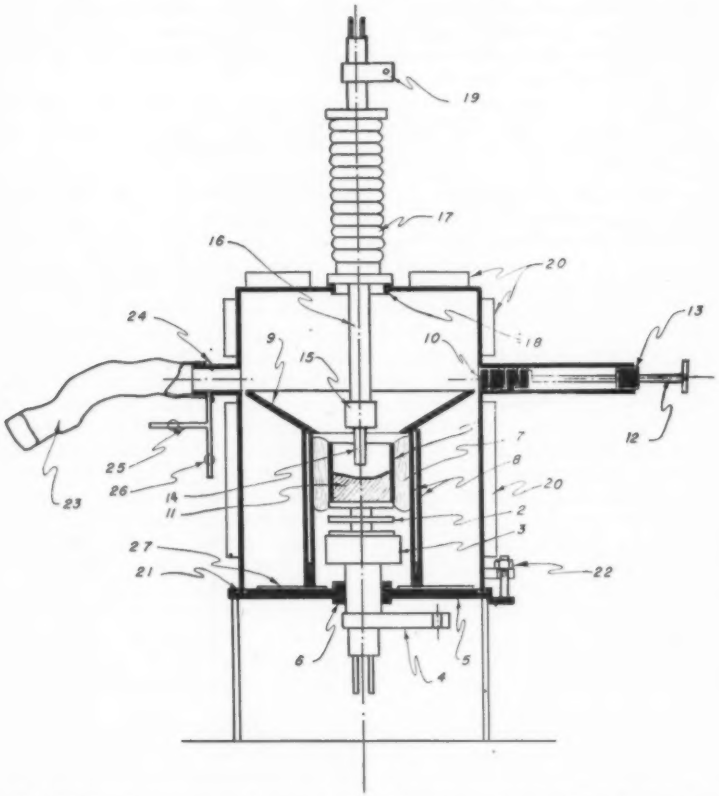

FIG. 1. Direct-current arc furnace. 1. Graphite sleeve; 2. graphite radiation screen; 3. water-cooled copper plug; 4. bus bar; 5. furnace bottom plate; 6. packing glands; 7. tungsten-wool insulation; 8. double radiation screen of graphite; 9. molybdenum funnel; 10. zirconium briquets; 11. melt; 12. pusher; 13. rubber stopper; 14. tungsten tip; 15. water-cooled plug; 16. copper pipe; 17. flexible tubing; 18. insulating packing gland; 19. copper connection plate; 20. water cooling; 21. rubber gasket; 22. bolts; 23. inner tube for gas expansion; 24. pipe stem; 25. stopcock to vacuum pump; 26. stopcock to helium tank; 27. asbestos plate.

introduction of more power with a given size of bus bar and a stirring effect in the crucible which aids considerably in preparing alloys. If desired, this type furnace can be operated under helium as well as in a vacuum.

The introduction of a heavy current through the furnace base presents a

problem. The base is made of brass or aluminum to avoid induction heating and through this base must be passed the necessary heavy, vacuum-tight leads for up to 4000 amperes current plus the necessary cooling water for cooling the connections with the graphite resistor. Some promise is shown in the design of rubber-to-metal bonded sleeves or plates which can be soft-soldered to the base and the power lead. Very large glass-to-metal seals could be used if available. We have preferred the standard electrode in-

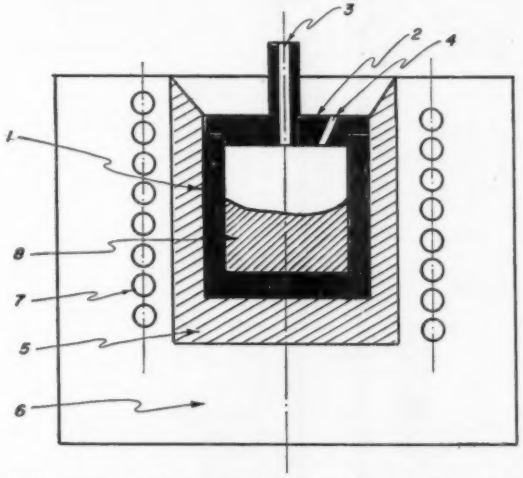

FIG. 2. High-frequency melting set-up. 1. Graphite crucible; 2. graphite cover; 3. graphite gas inlet; 4. gas escape and observing hole; 5. lampblack; 6. high-frequency furnace; 7. high-frequency coil; 8. melt.

troduction with ground artificial resin washers as vacuum seals, as shown in cross section in Fig. 3.

Casting of ingots by the bottom-plug method is particularly easy in the graphite-resistor furnace, since the bottom of the crucible is cooler because it is close to the water-cooled clamp. The plug, therefore, melts last. It has been found that a certain length of crucible will permit the plug to remain in place until the charge is completely melted. The plug then melts out automatically, and the molten charge runs into the mold below. A funnel is used to keep splashing metal from getting out into the furnace. The mold is slightly tapered and has a thin graphite disk in the bottom on which the metal stream impacts. When the ingot is knocked out of the mold, this disk, to which it is welded, comes with it. The arrangement of the furnace is shown in Fig. 4.

To recondition the crucible, it is necessary to saw off the button which remains on the pouring tip from the previous run to assure an undeflected stream on the next pour. The mold must be reamed to remove a thin film of adhering zirconium, which apparently forms there by evaporation. Crucibles can be used 15 to 20 times but the mold life at present is only

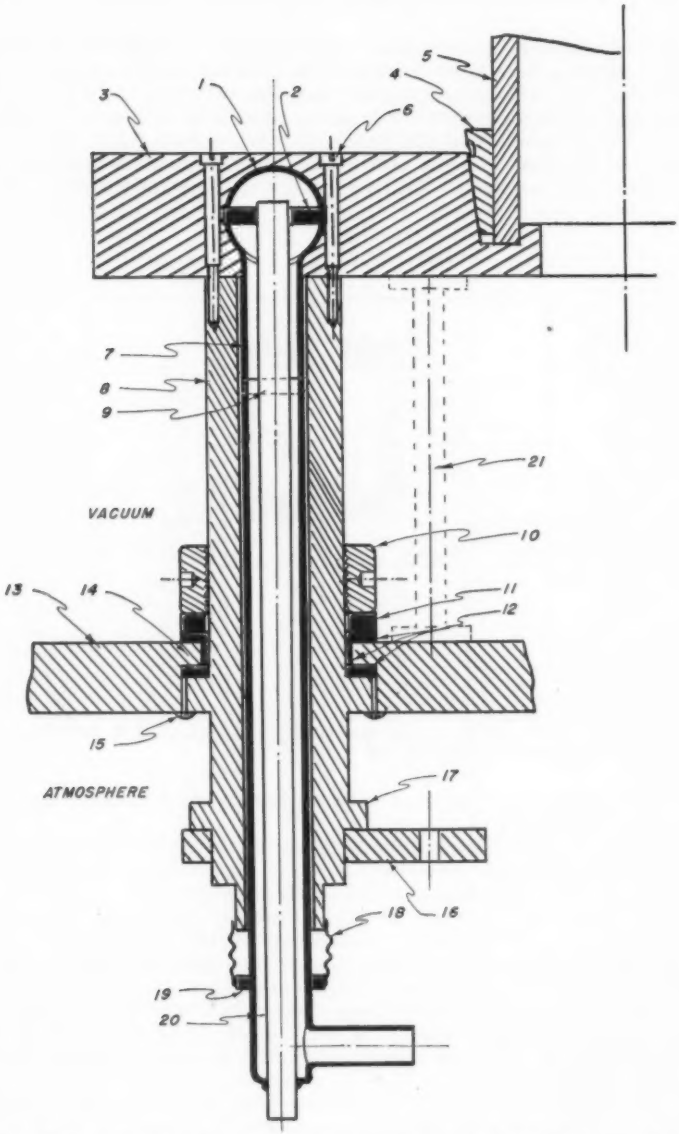

FIG. 3. Introduction of electrode. 1. Water jacket; 2. baffle; 3. copper clamp; 4. conus joint; 5. graphite-resistor tube; 6. screws; 7. outer pipe for water supply; 8. electrode shaft; 9. silver-soldered joint; 10. nut; 11. brass washer; 12. bakelite washers and sleeve; 13. brass base plate; 14. cut-down section; 15. grease; 16. bus bar; 17. brazed flange; 18. flexible bellow; 19. brass collar; 20. inner water-supply pipe.

about three runs. The crucible loses graphite to each charge and gradually becomes thin, as shown in Fig. 5. The usual carbon content of castings is 0.07–0.11 per cent, showing that the carbon pick-up of ingots is much lower than that of the metal frozen in the crucible, which is generally 0.17–0.25 per cent.

In vacuum, the single-phase carbon-resistor furnace melts 15 pounds of zirconium in 20 minutes with an average power input of 55 kw, which represents an energy consumption of 1.22 kwhr per pound. The carbon-

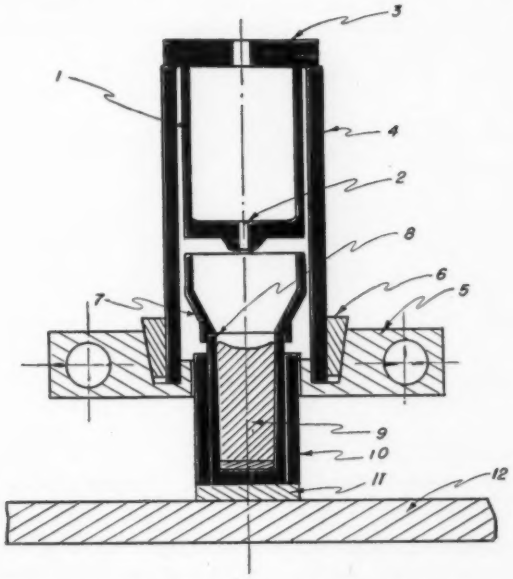

FIG. 4. Casting arrangement. 1. Graphite crucible; 2. tap hole; 3. cover; 4. graphite-resistor tube; 5. water-cooled clamp; 6. wedges; 7. graphite funnel; 8. graphite mold; 9. casting; 10. quartz; 11. quartz plate; 12. furnace bottom plate.

resistor furnace is well suited for melting in an inert gas, in which case the power consumption is considerably higher because of the higher dissipation of heat.

Spattering.—Sometimes a violent evolution of gas takes place during melting, and fused metal is driven upward in the crucible, where it freezes and forms skulls. This takes place both when melting in vacuum or under noble gas pressure. With the same batch of sponge, some melts boil, others do not. The evolution of gas in the moment of the eruption is only slight, as shown by the gauge, indicating that the products evolved are condensable, probably chlorides.

The analysis of the somewhat pyrophoric dirt collected in the furnace shell after many runs shows, besides zirconium, up to 8 per cent calcium

chloride, some manganese, and much magnesium and magnesium chloride. The calcium chloride originates from the 0.02–0.07 per cent calcium found in the commercial magnesium used in the reduction of the zirconium chloride. Calcium chloride has a much lower vapor pressure than magnesium chloride and it is not eliminated from the sponge when heated in vacuum at 900 C.

The causes of the boiling, when melting zirconium, are not yet clearly established. It is supposed, however, that the briquets, containing a small amount of chlorides, glaze over by superficial fusion, the core remaining rather cold because of the low heat conductivity of the metal. These glazed briquets float around the pool of fused metal until enough chloride pressure

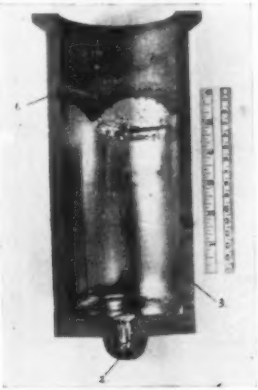

FIG. 5. Graphite crucible after fifteen melts, showing barely any corrosion. 1. Scar from torn-off skull; 2. plug; 3. surface glazed by zirconium.

builds up internally to make them burst. Liquid metal as well as unfused briquet material is now driven up into the top part of the crucible, where it freezes. Spattering when melting in an arc may have similar causes.

CONCLUSIONS

It has been shown that owing to the high melting point and chemical reactivity of zirconium and titanium, only graphite can be used as crucible material for producing large, commercial ingots. All refractory oxides either react or cannot be used commercially as crucible material.

Arc furnaces may be employed in vacuum or with inert atmosphere to build up ingots in a water-cooled copper mold or in graphite sleeves with varying amounts of contamination depending on electrode and crucible material.

High-frequency furnaces can produce large castings rather easily when inert atmospheres are employed. With certain restrictions, the same work may be done in vacuum. Use of graphite crucibles gives some contamination with carbon.

Split-tube, graphite-resistor furnaces are particularly suited to casting by the bottom-plug method to give uniform castings only slightly con-

taminated with carbon. The three-phase furnace shows stirring action of the bath. Castings with 0.07–0.11 per cent carbon are regularly obtained.

Experiments indicate that all three types of furnaces have distinct advantages and disadvantages. The choice as to which one is best depends partially upon the volume of gas to be tolerated in the ingot.

If fully degassed metal is desired, melting in the graphite-resistor vacuum furnace and casting give full satisfaction, especially with regard to low carbon content and freedom from residual hydrogen. High-frequency and arc vacuum furnaces for the production of castings are much more difficult to build and to operate.

Melting under a noble gas does not remove all the hydrogen contained in the metal, but may be entirely suitable for the production of zirconium that will not be used in electronics. The graphite-resistor, high-frequency, and arc furnaces are well adapted for this operation.

Any discussion of this paper will appear in the discussion section of Volume 96 of the Transactions of the Society.

REFERENCES

1. W. J. Kroll, *Trans. Electrochem. Soc.*, **78**, 35–47 (1940).
2. W. J. Kroll, U. S. Pat. 2,205,854, June 25, 1940.
3. W. J. Kroll, A. W. Schlechten, and L. A. Yerkes, *Trans. Electrochem. Soc.*, **89**, 263-276 (1946).
4. W. J. Kroll, A. W. Schlechten, W. R. Carmody, L. A. Yerkes, H. P. Holmes, and H. L. Gilbert, *Trans. Electrochem. Soc.*, **92**, 99 (1947).
5. W. J. Kroll, C. T. Anderson, and H. L. Gilbert, *Metals Technol.*, T. P. 2310 (1948).
6. W. J. Kroll, C. T. Anderson, H. P. Holmes, L. A. Yerkes, and H. L. Gilbert, *J.* (*and Trans.*) *Electrochem. Soc.*, **94**, 1–20 (1948).
7. J. H. de Boer, *Footeprints*, Vol. 3, No. 2, 18 (1930)—Reference: A. E. van Arkel, "Reine Metalle," p. 203, Springer (1934).
8. P. H. Brace, *J.* (*and Trans.*) *Electrochem. Soc.*, **94**, 170–176 (1948).
9. W. J. Kroll, *Z. anorg. Chem.*, **234**, 42–50 (1937).
10. W. C. Lilliendahl and H. C. Rentschler, *Trans. Electrochem. Soc.*, **91**, 285–297 (1947).
11. W. J. Kroll and A. W. Schlechten, *J.* (*and Trans.*) *Electrochem. Soc.*, **93**, 247–258 (1948).
12. W. von Bolten and Siemens-Halske, German Pat. 347,024 (1904) and 397,641 (1905); *Z. Elektrochem.* **11**, 45 (1905).
13. R. W. Moore, *Trans. Electrochem. Soc.*, **43**, 317–328 (1923).
14. M. Parke and J. L. Ham, *Trans. Am. Inst. Mining Met. Engrs.*, **171**, 416–430 (1947).
15. W. Espe and M. Knoll, "Werkstoffkunde der Hochvakuum Technik," p. 234, Springer (1936).
16. F. F. Poland, *Materials & Methods*, **23**, 710–712 (1946).
17. Heraeus Vakuumschmelze 1923–1933. Alberts Hofbuchhaltung, Hanau 1933, pp. 23–24.
18. W. Rohn, U. S. Pat. 2,133,634, Oct. 18, 1938.
19. Joost Rietveld and W. Ivory, Bios Final Report No. 1076, Item 21, PBL 78,259, p. 9.

THE DISSOLUTION OF ALUMINUM IN SODIUM HYDROXIDE SOLUTIONS. II[1]

MICHAEL A. STREICHER[2]

Lehigh University, Bethlehem, Pennsylvania

ABSTRACT

In continuation of a previous study (1) of the dissolution of commercially pure aluminum (99.2% Al) in alkaline solutions, the effect of impurities, concentration of sodium hydroxide, temperature, agitation, and the effect of an external current on the dissolution of a series of aluminum specimens ranging in composition from 99.2 to 99.998 per cent Al was investigated. Increasing quantities of impurities (iron being the most effective) increase the rate of dissolution. The largest increase is at the concentration of iron representing the limit of solubility of iron in solid aluminum. During the dissolution process the impurities in aluminum accumulate on the surface and accelerate the rate of dissolution.

An aluminum alloy containing 2.5 per cent Mg and 0.5 per cent Cr (52S) has a constant rate of dissolution. The impurities in this alloy, together with the alloying elements, drop to the bottom of the solution. They do not precipitate on the surface of the metal. The electrode potential for the alloy having a constant rate is constant, whereas the alloys whose rate of dissolution increases as the impurities precipitate on the surface reflect this increasing rate in electrode potential measurements, which change in the cathodic direction.

The rate of dissolution of aluminum reaches a maximum value as the concentration of sodium hydroxide is increased to 5.5*N*. At concentrations greater than 5.5*N* the rate of dissolution decreases. The decrease is linear with the concentration of sodium hydroxide between 7 and 12*N*. The effect of temperature on the rate of dissolution may be represented by the Arrhenius equation. The "experimental energy of activation" of this equation increases as the concentration of sodium hydroxide is increased up to 12*N*. Agitation equivalent to a linear velocity of 188 cm/sec does not change the rate of dissolution of the alloy containing Mg and Cr in 0.30*N* solution.

Making aluminum cathodic by means of an external current does not affect the electrode potential. The electrode potential changes observed on making aluminum anodic are correlated with measurements of the "difference effect."

An attempt is made to correlate the effect of increasing concentration of sodium hydroxide on the rate of dissolution with the specific conductance of the solution and to interpret the experimental results in terms of various electrochemical theories.

[1] Manuscript received February 11, 1949. This paper prepared for delivery before the Chicago Meeting, October 12 to 15, 1949.

[2] Present address: E. I. du Pont de Nemours & Company, Experimental Station, Wilmington, Delaware.

I. THE EFFECT OF IMPURITIES

Introduction

In a previous paper (1) the literature on the dissolution of aluminum in alkaline solutions was summarized. It was shown that the dissolution process in alkaline solutions was largely governed by an electrochemical mechanism similar to that observed in the case of some metals dissolving in acids with the liberation of hydrogen. For the previous study only commercially pure (99% Al) aluminum was used. It was found that the impurities in this metal accumulate on the surface during dissolution in sodium hydroxide and, by acting as cathodes of local cells, increase the rate of dissolution. In the present study, this effect of impurities in aluminum on the rate of dissolution in sodium hydroxide solutions has been further examined by extending the investigation to cover a series of alloys containing decreasing amounts of impurities.

TABLE I. *Analyses of alloys used*

Element	I	II	III	IV	V	VI
	Per cent of impurity					
Fe	0.0005	0.006		0.25	0.84	*
Cu	0.0005	<0.001		0.02	0.01	0.10
Si	0.001	0.002		0.15	0.14	*
Ti	—	<0.001		0.01	—	—
Mn	—	<0.001		—	—	0.10
Cr	—	<0.001		—	—	0.25
Mg	—	0.001		—	—	2.5
Zn	—	0.001		—	—	0.03–0.10
Al	99.998	99.99	99.97	99.57	99.01	96.50

* Fe + Max 0.45

IV, V, and VI are commercial alloys 1S, 2S, and 52S, respectively.

V—Typical composition of 2S alloy given by R. H. BROWN AND R. B. MEARS, *Trans. Electrochem. Soc.*, 74, 495 (1938).

VI—Typical composition of 52S given in "Metals Handbook," p. 820, 1948 Edition, A.S.M., Cleveland, Ohio, Rods obtained through courtesy of Mr. H. Adams, Aluminum Company of America, Allentown, Pa.

I—Original source: British Aluminium Co., Ltd. Specimens obtained through courtesy of Dr. M. Cohen, National Research Council, Ottawa, Canada, and Dr. W. Rostoker, University of Birmingham, England.

II and IV—Specimens and spectrographic analyses from Aluminium Laboratories, Ltd., Kingston, Ontario. Through courtesy of Dr. H. P. Godard.

III—Specimens obtained through courtesy of Mr. E. D. Verink, Jr., Aluminum Company of America, New Kensington, Pa.

Experimental Method

In Table I are given the analyses of the alloys used. With the exception of alloy VI, the aluminum content ranges from 99.0 to 99.998 per cent. The experimental procedure used was identical with that described in the previous paper. The specimens were punched in one piece from sheets 1 to 2 mm thick in the form of disks two inches (5.1 cm) in diameter with a $1\frac{1}{2}$ in. (3.8 cm) handle. The handle was covered with a plastic coating leaving an exposed area of 40.5 cm^2. The specimens were annealed at 360 C and were then allowed to dissolve in sodium hydroxide until the surfaces were uniform in appearance. All runs using 0.3*N* sodium hy-

droxide were made in 4 liters of solution, thus providing approximately 100 ml of solution per sq cm of aluminum surface. The solutions were placed in a constant-temperature bath. To eliminate the incubation and induction periods associated with the destruction of the oxide film, the specimens were immersed in concentrated (6*N*) sodium hydroxide solution until hydrogen bubbles appeared. The specimens were then rapidly withdrawn, rinsed immediately with water, and immersed in the test solution for a run.

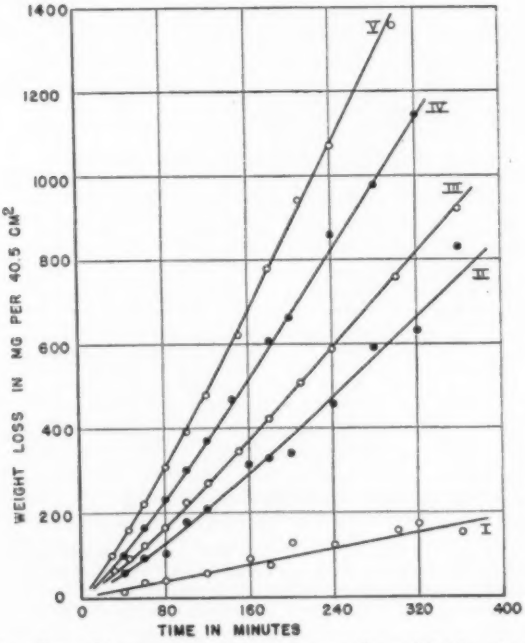

FIG. 1. The effect of impurities in aluminum on the weight-loss in 0.30*N* sodium hydroxide at 23 C.

Experimental Results

Weight-loss data for alloys I to V in 0.30*N* sodium hydroxide at 23 C have been plotted in Fig. 1. A large number of runs were repeated to obtain information on the reproducibility of dissolution rates. In general, for alloys III, IV, and V the maximum deviation from the arithmetic mean value did not exceed 3 per cent. For alloy II this increased to 8 per cent and for the highest purity metal (I) to 12 per cent. The decreasing reproducibility of the purer alloys is caused in part by the smaller weight-losses determined on them, which increase differences between identical runs on a percentage basis.

Specimens of highest purity aluminum (I) sometimes gave higher weight-losses than indicated in Fig. 1. Almost without exception, when the weight-loss did not fall in the region of line I, it fell in the region of line II rather than between these two curves. Whenever alloy I gave weight-losses of the magnitude of alloy II, a precipitate was observed on the surface of the specimen. This precipitate was formed on all specimens except in the case of alloy I when it gave values of line I (Fig. 1). In some instances, the quantity of precipitate formed during a run was found to be so small that it was not visible unless a part of the surface of the specimen was wiped. The resulting contrast between the wiped and the untouched surface revealed the precipitate.

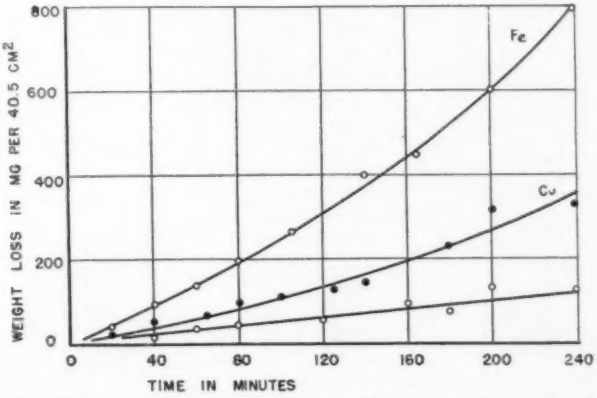

FIG. 2. The effect of impurities ($FeCl_3$ and $CuCl_2$) in the solution on the dissolution of alloy I in 0.30*N* sodium hydroxide at 23 C.

As the quantity of impurities in the alloy is increased, the rate of dissolution increases. Whenever a precipitate forms on the surface, the rate of dissolution increases with the time of immersion. The rate increases at a decreasing rate approaching a constant rate of dissolution after about 160–200 minutes.

In order to determine the effect of impurities in the solution, a series of runs was made using alloy I in solutions to which iron and copper had been added. For these runs a small quantity of cupric chloride or ferric chloride was dissolved in distilled water. This solution was then added to the 0.30*N* sodium hydroxide. A precipitate of iron or copper hydroxide is formed, which settles at the bottom of the solution. In this way a small but constant supply of iron or copper ions is provided. The data obtained with highest purity aluminum (I) in solutions containing copper or iron, along with the weight-losses obtained without additions to the solution, are plotted in Fig. 2.

Both copper and iron in the solution increase the rate of dissolution of highest purity aluminum by cementation. An almost invisible precipitate is produced in solutions containing iron, while in the solutions containing

copper, a relatively heavy sludge is formed on the aluminum surface. Thus, a very small precipitate of iron has a considerably greater effect on the rate of dissolution than does a heavy precipitate of copper. This fine precipitate of iron from the solution increases the rate of dissolution of highest purity aluminum (I) by a factor of eight and results in a weight-loss after 240 minutes of the magnitude of alloy IV (Fig. 1), which contains 0.25 per cent iron. The rate of dissolution of alloy I in solutions containing iron continues to increase up to 240 minutes, while impurities, when added to the metal, result in an (increasing) rate of dissolution which approaches a constant value.

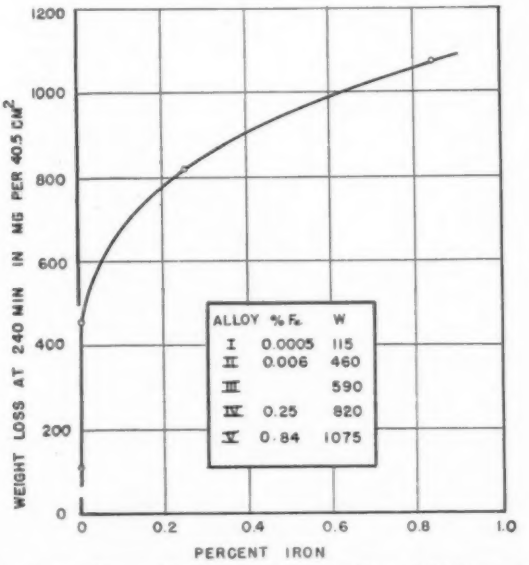

FIG. 3. The effect of impurities in aluminum on the weight-loss in 0.30*N* sodium hydroxide at 23 C. Weight-loss at 240 minutes taken from Fig. 1.

The principal impurities in the alloys (I–V) used in this study are iron, copper, and silicon. Of these, iron is usually present in the largest amount (Table I). As shown above, iron is considerably more effective in increasing the rate of dissolution of aluminum in sodium hydroxide than copper (Fig. 2). This has also been observed by Straumanis and Brakšs (2) and by v. Zeerleder and Zurbrügg (8) in the case of aluminum alloys containing iron or copper as alloying elements. Quantities of silicon of the order of 0.1 per cent have only a very slight effect on the dissolution of aluminum in sodium hydroxide (3, 8). Therefore, iron is the most effective impurity in accelerating the rate of dissolution of those present in the alloys studied. In Fig. 3 the weight-loss after 240 minutes of immersion in 0.30*N* sodium hydroxide at 23 C has been plotted against the per cent of iron in the various alloys.

Discussion

When the data of Fig. 1 for the interval of increasing rates of dissolution are plotted on logarithmic coordinates, linear relationships are obtained. Therefore, these data may be represented in the range before a constant rate is reached, i.e., up to 160–240 minutes, by an equation of the type

$$W = at^b \qquad (I)$$

where W is the weight-loss in mg per 40.5 cm^2, t, the time of immersion in minutes, and a and b are constants. In the previous study (1) on commercially pure aluminum (V), it was found that a varies with the temperature and concentration of the solution, while $b = 1.11$ is independent of these variables. A graphical determination of b for alloys II, III, and IV gave 1.16, 1.11, and 1.18, respectively. Thus, since these variations are within the experimental error, b also appears to be independent of the quantity of (iron) impurities present in the alloys. The constant a varies with the concentration of impurities (iron) in the alloys in a similar manner, as indicated for the weight-loss in Fig. 3.

The effect of impurities on the dissolution of aluminum in alkaline solutions has been studied by a number of investigators (2, 4–13, 21). Straumanis and Brakšs (2) found that increasing additions of iron or copper (beginning with 0.01 %) alloyed with highest purity aluminum increase the rate of dissolution. The accelerating effect was most pronounced for small quantities and fell off rapidly as increasing quantities of iron or copper were added. Iron was more effective than copper in increasing the rate. It was found by v. Zeerleder and Zurbrügg (8) that, after an initial increase in the rate of dissolution of highest purity aluminum as copper or iron are added as alloying elements, there is no further increase when these elements are added in quantities greater than 0.10 per cent iron or 0.15 per cent copper. These authors made two series of runs. Aluminum containing various quantities of impurities was annealed at 500 C for one series of runs and at 300 C for another. It was assumed that the annealing treatment at 500 C resulted in a homogeneous structure and at 300 C in a heterogeneous structure (14). The fact that the dissolution rates in sodium hydroxide appeared to be unaffected by these thermal treatments and by quantities of iron and copper over 0.10 per cent and 0.15 per cent, respectively, led Schenk (14) to conclude that the process of dissolution in alkaline solutions is not governed by the formation of local cells, but by the rate of dissolution of a constantly forming aluminum hydroxide film.

In a recent determination of the solubility of iron in solid aluminum, Edgar (15) found that the solubility of iron decreases from 0.052 per cent at the eutectic temperature (655 C) to 0.006 per cent at 500 C.[3] In the present study, the largest increase in the rate of dissolution was found between alloy I (0.0005% Fe) and alloy II (0.006% Fe) (Fig. 3). It was also observed that, when alloy I gave higher weight-losses than indicated in Fig. 1, these were in the range of alloy II rather than between the values obtained for these two alloys. These observations seem to indicate that there is a sudden increase in the rate of dissolution when a second phase

[3] Therefore, only those alloys containing less than 0.006 per cent iron are subject to homogenization at 500 C. Only one alloy of the iron series used by (8) contained less than this amount.

appears.[4] The rate continues to increase with increasing iron content after the second phase appears, but much more slowly.

A very thin precipitate of iron, produced on highest purity aluminum (I) by the addition of iron to the solution, produces an effect on the weight-loss equivalent to that resulting from 0.25 per cent iron alloyed with aluminum (alloy IV), primarily in the form of a second phase. This alloy forms a much heavier sludge, which has a sponge-like structure when viewed under the microscope. If the assumption that the aluminum iron-compound is insoluble in alkaline solutions is justified, this would indicate that iron is considerably less effective when present in combined form accumulating on the surface than is redeposited iron, which may have entered the solution when the aluminum-iron solid solution dissolved. Since the solubility of iron in solid aluminum is very small, the amount of redeposited iron, though very effective in increasing the rate, will never be very large.

There appear to be a number of ways in which iron increases the rate of dissolution of aluminum in alkaline solution:

1. Iron in aluminum solid solution dissolves and precipitates on the aluminum surface where it is then very effective in increasing the rate of dissolution.
2. When the iron content of aluminum is increased to the concentration where a second phase appears, there is a sudden increase in the rate of dissolution of the metal.
3. An increase in the amount of the second phase increases the rate of dissolution, but the rate of increase falls off with increasing amounts of the second phase.
4. When aluminum containing a second (iron-aluminum) phase dissolves, this phase (assuming that it is insoluble in alkaline solutions) accumulates on the surface forming a sludge which increases the rate of dissolution. However, the effectiveness of this sludge in increasing the rate of dissolution is considerably less than that of precipitated iron.

II. THE EFFECT OF CONCENTRATION OF SODIUM HYDROXIDE

Introduction

When the concentration of sodium hydroxide is increased to 1*N* or greater, a precipitate is formed on highest purity aluminum (I), which increases the rate of dissolution with time in a manner similar to that observed on aluminum containing larger quantities of impurities. Whether this accumulation of impurities on the surface of highest purity aluminum is a result of the larger weight-losses obtained in more concentrated solutions or is caused by impurities in the sodium hydroxide used could not be determined.[5] At concentrations of 6*N* and greater, this precipitate flakes off, and, as a result, the rates obtained below this concentration are not comparable with those determined above this concentration.

In order to obtain dissolution rates which were comparable over the

[4] The second phase corresponds approximately to the formula $FeAl_3$ (16).

[5] Reagent grade sodium hydroxide, whose maximum limits of impurities were 0.002 per cent for Fe and 0.003 per cent for heavy metals (as Ag), was used. These impurities may become effective when large quantities of sodium hydroxide are used for concentrated solutions.

entire range of concentration of sodium hydroxide studied, alloy VI, containing 2.5 per cent magnesium and 0.5 per cent chromium added to commercially pure aluminum (V), was used. During the dissolution process the impurities, copper, iron, or compounds, do not form a precipitate on the specimen but fall to the bottom of the solution. Therefore, the rate is constant with the time of immersion, and the problem of determining the effect of concentration of sodium hydroxide on the rate of dissolution is somewhat simplified.

Experimental Results

Alloy I.—Only one liter of solution was used for runs in solutions over 1*N*. Some of the data on the effect of increasing concentration of sodium

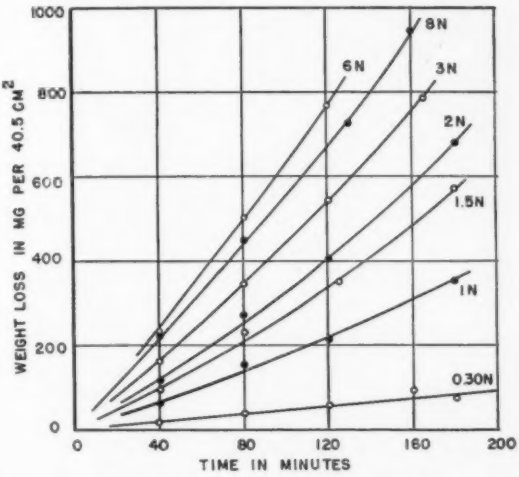

FIG. 4. The effect of concentration of sodium hydroxide on the dissolution of alloy I at 23 C.

hydroxide on the weight-loss of highest purity aluminum are plotted in Fig. 4. The rate of dissolution increases with time. When the data are plotted on logarithmic coordinates, linear relationships result. Therefore, equation (I) may also be used to describe this case of the effect of impurities on the rate of dissolution. The constant b for each concentration of sodium hydroxide studied was determined from the logarithmic plot. By differentiating equation (I) with respect to time and substituting for a, equation (Ia) is derived.

$$\frac{dw}{dt} \frac{W^b}{t} \qquad \text{(Ia)}$$

The rates of dissolution at 100 minutes of immersion can now be calculated by substituting values of b obtained from the logarithmic plot of W vs. t. These rates have been plotted in Fig 6.

At the higher concentrations, the effect of the precipitate is uncertain because it sometimes flakes off during a run. For example, at $7N$ the weight-loss was found to be linear with time of immersion, ($b = 1.00$), indicating that, in this case, the precipitate was not active. The rate of dissolution reaches a maximum in about $5N$ sodium hydroxide, and in concentrations greater than $5N$ begins to decrease.

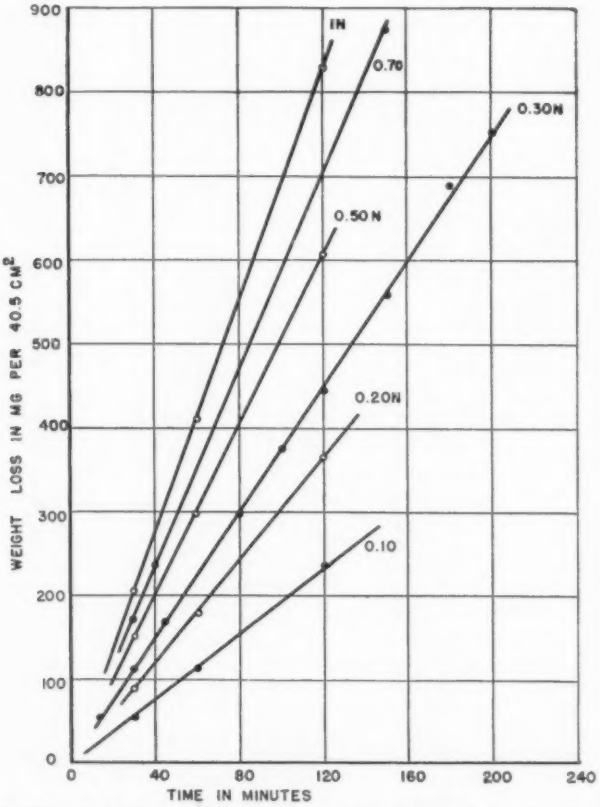

FIG. 5. The effect of concentration of sodium hydroxide on the dissolution of alloy VI at 23 C.

Alloy VI.—The weight-loss data of alloy VI are plotted in Fig. 5 for concentrations up to $1N$. The data for concentrations greater than $1N$ are given in Table II. The reproducibility of these weight-losses is better than that of any of the other alloys studied. The maximum deviation from the arithmetic mean is less than one per cent. A linear relationship between weight-loss and time of immersion was found at all concentrations of sodium hydroxide.

TABLE II. *Weight-loss of alloy VI in solutions of sodium hydroxide greater than 1N at 23 C*

N	Weight-loss in mg/40.5 cm²	
	15 min	30 min
1.50	121.1	246.2
2.0	144.0	274.5
4.0	166.7	333.0
5.0	172.3	343.4
6.0	173.8	343.0
7.0	165.0	331.9
8.0	155.7	302.2
9.0	144.3	287.1
10.0	134.0	264.7
12.0	114.1	224.7

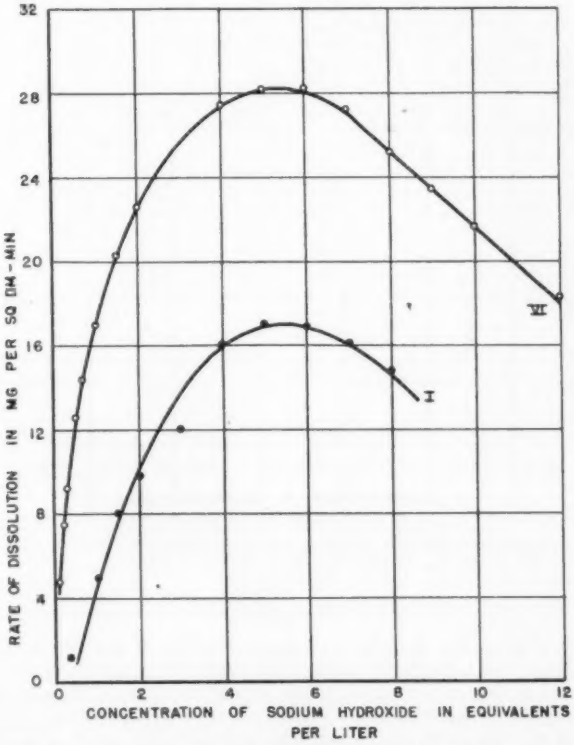

FIG. 6. The effect of concentration of sodium hydroxide on rate of dissolution of alloys I and VI at 23 C.

During the dissolution of alloy VI (52S) the impurities do not accumulate on the surface, but drop to the bottom of the solution along with hydroxides of the alloyed magnesium and chromium. As a result, there is no accelerating action of the impurities by precipitation on the surface, and the rate of dissolution remains constant. Electrode potential measurements described in Section IV provide further evidence of this process.

The rates of dissolution determined by evaluation of the slope of the weight-loss-time lines were converted to mg/100cm²/min and plotted in Fig. 6. The rate of dissolution of alloy VI increases with increasing concentration of sodium hydroxide until a maximum value is reached at about 5.5*N*. From this point on, the rate decreases with increasing concentration. This decrease is linear between 7 and 12*N*. The rate of dissolution in 12*N* is approximately the same as in 1.2*N* solution.

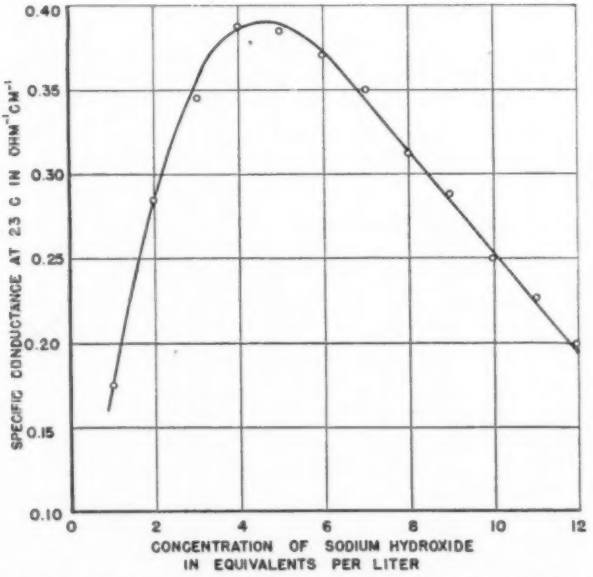

FIG. 7. Specific conductance of sodium hydroxide solutions at 23 C interpolated from data given in the literature (17).

Discussion

Previous studies on the effect of concentration of sodium hydroxide on the dissolution of aluminum have been made by Centnerszwer (4), who concluded that the rate of dissolution is proportional to the square root of the hydroxyl ion concentration in solutions up to 1*N*. Gadeau (5) gives the weight-loss of aluminum alloys containing various amounts of impurities in solutions up to 2.5*N*, with a maximum weight-loss at 1.2*N*. In the previous study (1), the effect of concentration of sodium hydroxide on the dissolution

of alloy V was represented in the range of 0.10–0.50N by the empirical equation

$$W = kC^d \qquad \text{(II)}$$

where W is the weight-loss in mg, C, the concentration in milliequivalents per liter, and k and d are constants. The constant k was found to vary with temperature and length of time of immersion, while (d = 0.46) appeared to be independent of these variables.

From data in the literature (17) on the equivalent conductance of sodium hydroxide at various concentrations and temperatures, the values at 23 C were interpolated graphically. These values were then converted to specific conductance and plotted in Fig. 7. The specific conductance increases with increasing concentration of sodium hydroxide to a maximum value at

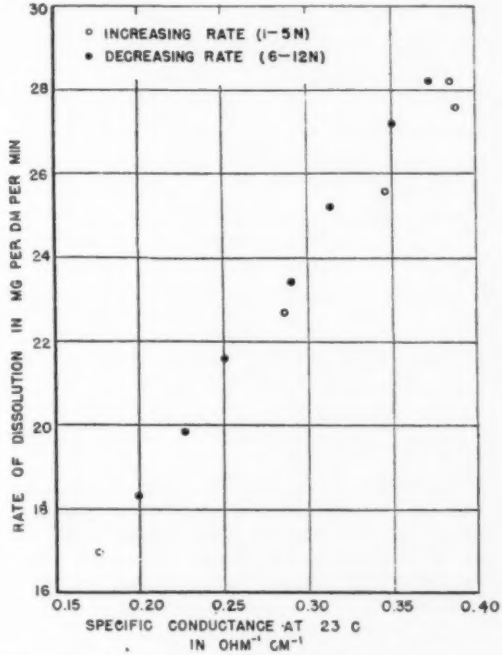

FIG. 8. Rate of dissolution of alloy VI *vs.* specific conductance of sodium hydroxide at 23 C.

about 4.5N. From this point on, the specific conductance decreases with increasing concentration. The decrease is linear between 7 and 12N. In Fig. 8 are plotted the rates of dissolution of alloy VI against the specific conductance for solutions 1N and over. The data on the effect of temperature on the equivalent conductance of solutions below 1N do not permit interpolation at 23 C.

Since the concentration of sodium hydroxide at the maximum rate of dissolution (5.5*N*) does not coincide with that at which the specific conductance is a maximum (4.5*N*), there is some scatter among the values in Fig. 8 representing 4–6*N* solutions. Because both the rate of dissolution and the specific conductance are linear with the concentration between 7–12*N*, a linear relationship results in Fig. 8 between the values representing this range of concentrations.

III. THE EFFECT OF TEMPERATURE AND AGITATION ON ALLOY VI

Temperature

The rates of dissolution of alloy VI at various temperatures and concentrations of sodium hydroxide were found. The weight-loss data are given in Table III. The dissolution of alloy VI is constant with time of

TABLE III. *The effect of temperature on the weight-loss of alloy VI*

Time in minutes	Temperature in C			
	23	26	33	40
		0.30*N*		
15	56.1	—	—	—
30	114.6	143.2	215.9	—
45	171.2	217.3	321.4	476.7
60	—	285.4	429.8	630.6
		5*N*		
15	172.3	201.8	329.9	—
30	343.4	415.3	665.3	—
		12*N*		
15	114.1	143.7	257.7	—
30	224.7	293.0	518.7	—

immersion at all temperatures studied. From the weight-loss data the rates of dissolution were calculated, and the logarithm of the rate of dissolution was plotted against the reciprocal of the absolute temperature in Fig. 9. At all three concentrations studied, linear relationships were found. The effect of temperature on the rate of dissolution may, therefore, be given by the Arrhenius equation

$$\frac{dw}{dt} = Ae^{-E/RT} \qquad \text{(IV)}$$

where R is the gas constant, E is the "experimental energy of activation," and A is a constant which is independent of the temperature (18). From the slopes of the lines in Fig. 9 the values of E were calculated in calories per mole. These values are given in Fig. 9. The "experimental energy of

activation" increases with increasing concentration of sodium hydroxide up to 12N, in contrast to the rate of dissolution, which passes through a maximum at 5.5N.[6]

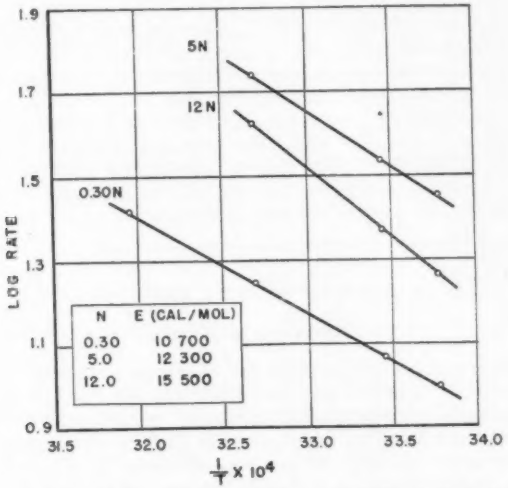

FIG. 9. The effect of temperature on the rate of dissolution of alloy VI

TABLE IV. *The effect of agitation on the rate of dissolution of alloy VI in 0.30N sodium hydroxide at 23 C*

Time in minutes	Weight-loss in mg/40.5 cm²		
	No agitation	380 rpm*	2880 rpm
40	174	172	—
60	254	—	252
70	—	304	—
80	—	—	—
90	390	395	—
120	514	528	—

* Diameter of specimen = 1.25 cm.

Agitation

A number of specimens of alloy VI in the form of rods (d = 1.25 cm) were used to study the effect of agitation on the rate of dissolution. A constant speed motor in combination with gears provided rotational

[6] The value of 13,700 cal/mole was found for alloy V in the range of 0.10–0.50N sodium hydroxide (1).

speeds up to 2880 rpm.[7] The bottom of the rod and the area near the water line were given a coating leaving approximately 20 cm² free. The exposed areas were carefully measured in each case, and the weight-losses were converted to mg/40.5 cm². Weight-losses were first determined without agitation (Table IV). The weight-loss is linear with the time of immersion as in the case of sheet specimens (Fig. 5), but the rate of dissolution is somewhat greater than that obtained for sheet specimens. This is probably the result of slight variations in the composition of this commercial alloy (52S) between sheet and bar stock or different lots.

As shown in Table IV, agitation equivalent to a linear velocity of 188 cm/sec (2880 rpm) does not affect the rate of dissolution. The absence of any effect of agitation on the rate of dissolution and the temperature coefficient of approximately two (R_{t+10}/R_t) indicate that diffusion processes probably do not control the rate of dissolution under freely dissolving conditions.

IV. ELECTRODE POTENTIAL MEASUREMENTS

Experimental Results

The experimental procedure used for electrode potential measurements was the same as that previously described (1). In Fig. 10 are given the electrode potential measurements obtained with various alloys used. The values obtained on alloy I are given in Fig. 11. All electrode potential measurements given in Fig. 10 are reproducible. The curve for alloy I (Fig. 11) is a typical example of those obtained for this alloy. The more or less constant potential obtained after about 40–120 minutes varies between −1.95 and −2.00 volts (0.1*N* Calomel Scale). Data representing the effect of additions of iron or copper ions to the solution on the electrode potential of alloy I are also given in Fig. 11.

The electrode potentials of alloys, which form a precipitate on the surface during dissolution, change in the cathodic direction during the dissolution process. As the quantity of impurities in aluminum is increased and the rate of dissolution increases, the electrode potential becomes more cathodic.[8] An electrode potential run was made using an aluminum alloy (24ST) containing 4.5 per cent copper, 0.6 per cent manganese, and 1.5 per cent magnesium, in addition to the impurities contained in commercially pure aluminum (V). It was found that the potential-time curve of this alloy practically coincided with that obtained for alloy V (2S).

In those cases in which a precipitate forms on alloy I as a result of a high sodium hydroxide concentration, the electrode potential is more cathodic and changes in the cathodic direction with immersion-time in a similar manner as observed on alloys containing larger quantities of impurities. This was also found to be the case when alloy I gave weight-losses in the region of alloy II. The electrode potentials of alloy VI are constant with immersion-time at various temperatures and are reproducible.

[7] The writer is indebted to Mr. Bernt Roald, Lehigh University, for the use of this apparatus.

[8] Brown, Fink, and Hunter (19) found that increasing quantities of copper change the electrode potential of aluminum in a sodium chloride-hydrogen peroxide solution to more cathodic values and used this phenomenon to derive the solubility curve of copper in solid aluminum.

Discussion

In the previous study (1), it was shown that the change in electrode potential is related to the formation of the precipitate on the surface, which increases the rate of dissolution. Whenever a precipitate was observed on the alloys studied, there was a corresponding change in the electrode potential with time of immersion (alloys II, III, IV, and V). In the case of

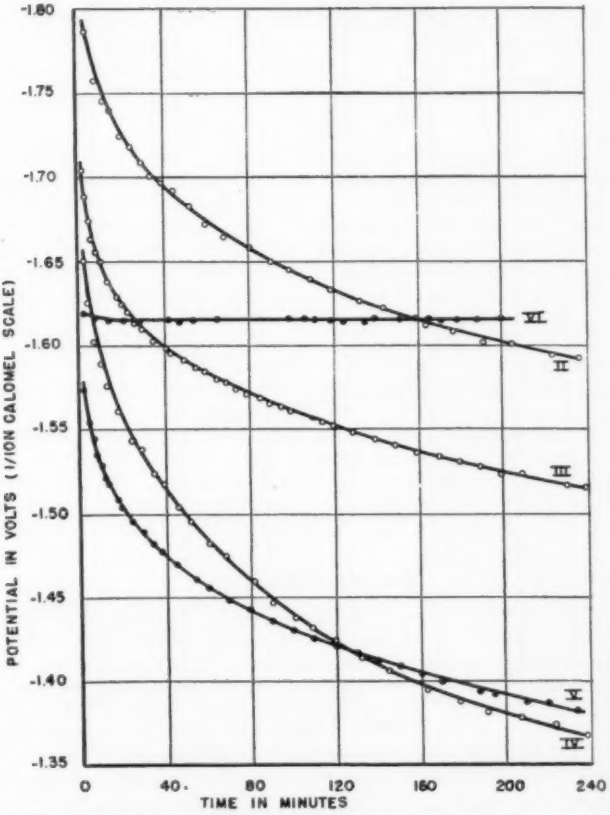

FIG. 10. The effect of time of immersion on the electrode potential of alloys II–VI in 0.30*N* sodium hydroxide at 23 C.

alloy VI, the precipitate did not form on the surface but fell to the bottom of the solution. The rate of dissolution and, therefore, the electrode potential are constant with time of immersion. An increase in the rate of dissolution, whether brought about by the accelerating action of impurities accumulating on the surface or by alloying elements, results in a change toward more cathodic electrode potentials. This is in agreement with the results of Müller (10) and Straumanis (2).

Iron or copper compounds added to the solution not only cause an increase in the rate of dissolution of highest purity aluminum (I), but also cause a progressive change in electrode potential in the cathodic direction.

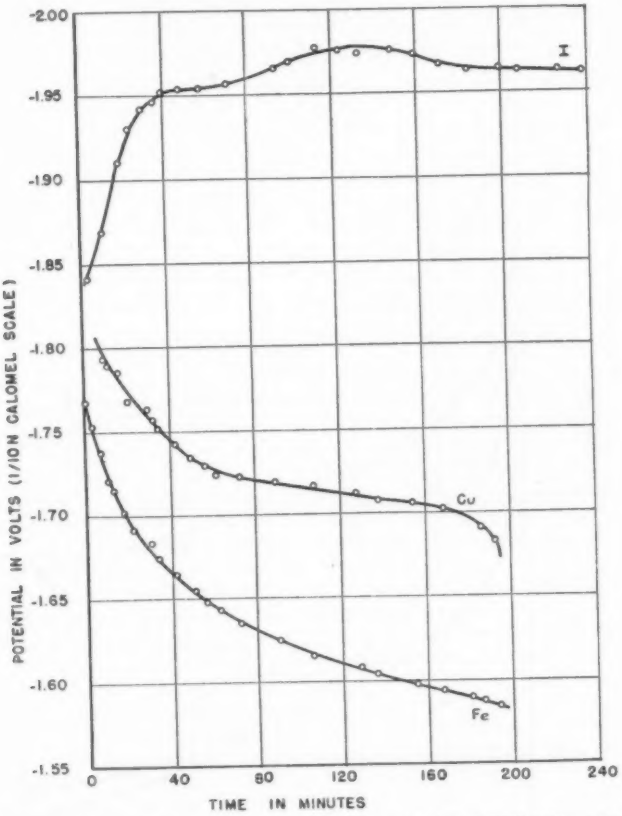

FIG. 11. The effect of iron and copper chlorides added to 0.30*N* sodium hydroxide solution on the electrode potential of alloy I at 23 C.

V. THE EFFECT OF AN EXTERNAL CURRENT

Introduction

Considerations in connection with a previous investigation on the "difference effect"[9] of alloy V indicated that this effect is a result of anodic

[9] The (positive) "difference effect," first described by Thiel and Eckell (23), is defined as the decrease in local cell action on an electrode made anodic in a corroding solution by means of an external current. This decrease is often linear with the externally applied current. The total corrosion, consisting of local cell corrosion and corrosion as a result of the external current, is increased by the external anodic current.

polarization by an external current. Changes in electrode potentials measured on an aluminum specimen containing impurities, which precipitate on the surface while the specimen is made an anode by an external current, are a function of the change in potential produced by both the external current and by the local cell action of precipitated impurities. Therefore, it is difficult to determine the effect of an external current on the electrode potential of such a specimen. In an effort to avoid this difficulty, such measurements were made on alloys I and VI. Alloy I contains a minimum of impurities, while the impurities in alloy VI are prevented from precipitating on the surface and thus do not interfere with electrode potential measurements.

Experimental Method

The circular specimens used for weight-loss runs were covered on one side with a plastic coating leaving a surface area of 20.3 cm^2 uncoated. Facing the uncoated side was placed a copper electrode of identical dimensions and also coated on the reverse side. The distance between the uncoated faces was kept constant throughout a run and was about 6.5 cm. For electrode potential measurements, a glass tubulus was brought as near to the surface of the aluminum specimen as was possible without forcing the hydrogen evolved on the aluminum into the tubulus. For any run, the distance between the aluminum specimen and the tubulus was held constant. The source of external current was a d-c generator. By adjusting a series of resistances, the current to the aluminum electrode was determined and held constant.

The current density on the aluminum specimen was increased gradually in small intervals by varying the external resistances. At each setting of current density, the electrode potential was measured with a potentiometer and the potential drop across the copper and aluminum electrodes was determined by means of a voltmeter.

Experimental Results

The results of electrode potential measurements on alloy I while under the influence of an external current are plotted in Fig. 12. The electrode potential of alloy I changes linearly to more cathodic values with increasing anodic current density up to 0.2 amp/20.3 cm^2 in 0.30*N* solution. At this current density hydrogen evolution at the anode, which gradually decreases with increasing current density, ceases, and there is a change in slope. It was found that the rate at which the external current was applied influenced the electrode potential. When the external current is increased in relatively small intervals, the corresponding potentials are constant and do not fluctuate, while large increases in external current result in fluctuating potentials.

The current density required to suppress hydrogen evolution was reproducible at 0.20 amp/20.3 cm^2 in 0.30*N* solution. From about 0.35 amp on, the potential changes rapidly and is no longer linear. The voltage drop across the aluminum-copper couple is linear with the current density up to approximately the same current density (Fig. 14). In 8*N* solution a current density of 0.70 amp/20.3 cm^2 is required to suppress hydrogen evolution, and the slope of the potential curve also changes at this point.

When aluminum (alloy I) is made the cathode, there is no change in electrode potential up to 0.32 amp/20.3 cm², and then there is a slight increase in the more anodic direction to somewhat fluctuating values. The corresponding voltmeter readings are linear with the current density and range from 2.6 to 3.8 volts.

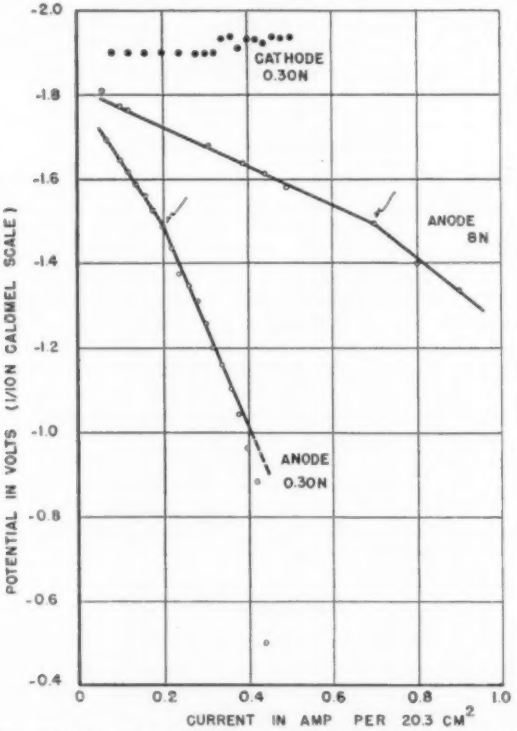

FIG. 12. The effect of an external current on the electrode potential of alloy I at 23 C. Arrows indicate cessation of hydrogen evolution.

The polarization data for alloy VI are given in Fig. 13. Again, when aluminum is made the cathode there is no change in electrode potential as the current density is increased up to 0.25 amp/20.3 cm². At higher values there is a slight change in potential in the anodic direction. This change (also in the case of alloy I) may be a result of the vigorous evolution of hydrogen on the surface of the specimen. The concentration of sodium hydroxide does not change the potential, while the specimen is made a cathode. The voltmeter readings are linear with the current density and vary from 2.6 to 3.6 volts.

When alloy VI is made an anode by means of an external current there is

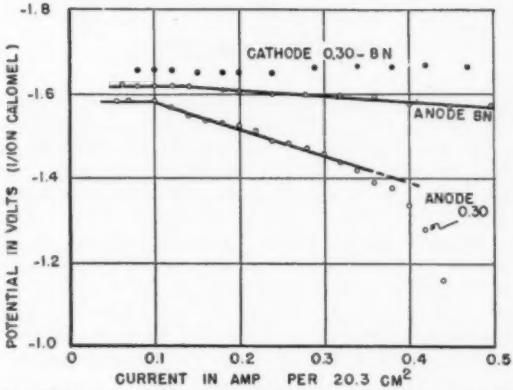

FIG. 13. The effect of an external current on the electrode potential of alloy VI at 23 C.

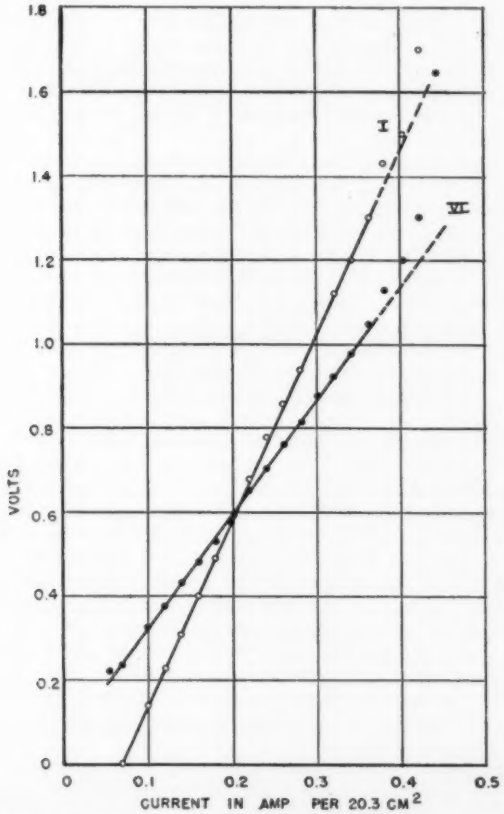

FIG. 14. Potential drop across copper-aluminum electrodes as the external current is increased in 0.30*N* sodium hydroxide solutions at 23 C (aluminum = anode).

at first no change in electrode potential up to 0.10 amp/20.3 cm^2 in 0.30*N* solution and up to 0.15 amp in 8*N* solutions. From this point on, there is a linear change to more cathodic potentials as the current density is increased which is more rapid in 0.30*N* than in 8*N* solution. At 0.42 amp in 0.30*N* solution, hydrogen evolution ceases on the anode and an adherent film is formed. In 8*N* solution a current density of about 1.2 amp/20.3 cm^2 is required to suppress hydrogen evolution (not shown in Fig. 13). The electrode potential is approximately the same at this point as in 0.30*N* solution when hydrogen evolution ceases. The voltage across the Al-Cu couple is linear with the current density up to 0.35 amp (Fig. 14), which is about the same current density at which the electrode potential in 0.30*N* solution departs from a linear relationship with the current density (Fig. 13).

Discussion

Potential measurements on aluminum dissolving in sodium hydroxide solutions under the influence of an external anodic current have been made by a number of investigators (2, 10, 20–22). Straumanis (2) has shown at relatively low current densities (up to 5 ma/cm^2 in 0.5*N* solution) that the electrode potential is linear with the current density. This has led to the conclusion that the positive "difference effect" is a result of anodic polarization produced by the external current (1, 2) which reduces the potential difference of the local cells.

In the previous investigation, the effect of an external current on the dissolution of alloy V in 0.30*N* solution was determined. Fig. 15 gives a plot of the data obtained together with a schematic representation of the corresponding changes in electrode potential derived from measurements on alloys I and VI (Fig. 13 and 14). Since impurities precipitating on the surface of alloy V complicate electrode potential measurements while it is being made anodic by an external current, it was necessary to derive a schematic electrode potential curve for it from measurements on alloy VI, which contains similar impurities (Fe, Cu) as alloy V, and alloy I, whose electrode potential at the limiting value of the "difference effect" is not complicated by the formation of a visible, adherent film as in the case of alloy VI.

An external, anodic current does not have any effect on the weight-loss of alloy V (containing about 1% of impurities) up to a current density of 7 ma/cm^2 in 0.30*N* solution at 23 C (1). Similarly, the electrode potential of alloy VI, containing approximately the same impurities in addition to magnesium and chromium, remains constant up to a current density of 5 ma/cm^2. At higher current densities the "difference effect," i.e., a decrease in local cell action, is observed, which reaches its limiting value at a current density, *r*, (Fig. 15). At this point, local cell action has been suppressed, and there is no hydrogen evolution on the aluminum surface. The weight-loss is now electrochemically equivalent to the external current. For alloy V the current density required to reach this point was 27 ma/cm^2, and for alloy VI it was 21 ma/cm^2. Thus, the current densities at which changes in slope take place on the weight-loss and potential curves of Fig. 15 are in approximate agreement.

Electrode potential measurements are linear with the current density in the range of the "difference effect" almost throughout the entire range for

alloy VI. When the limiting value is approached, there is some deviation (also in the voltmeter readings), which coincides with the formation of an adherent film. For alloy I, which contains no magnesium or chromium, the potential is linear with the current density throughout the entire range (Fig. 12), as is the potential difference between the aluminum and the copper electrode.

When hydrogen evolution is suppressed on the anode by an external current, the weight-loss is electrochemically equivalent to the external current. Thus, for alloy I (Fig. 12) it should be possible to calculate the weight-loss from the quantity of external current measured with an ammeter over a given period of time at a current density over 0.20 amp/20.3 cm^2 in 0.30*N* solution at 23 C. A run was made at 0.30 amp and the weight-loss was determined and calculated: $W_{obs.} = 154$ mg, $W_{calc.} = 151$ mg.

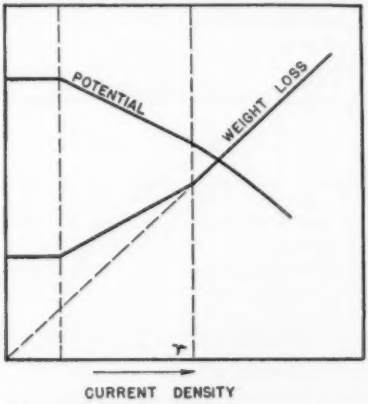

FIG. 15. The effect of an external anodic current on the dissolution of alloy V in 0.30*N* sodium hydroxide at 23 C. Weight-loss curve from (1) and schematic potential curve derived from measurements on alloy I and alloy VI.

In the previous investigation it was found, in agreement with Caldwell and Albano (26), that making aluminum cathodic in alkaline solution does not affect the rate of dissolution appreciably. As shown in Fig. 12 and 13, there is practically no change in potential when aluminum is made cathodic by means of an external current. These findings are in agreement with the theory of cathodic protection of Brown and Mears (25), who have shown that cathodic polarization (to the open circuit potential of the local anodes) is necessary to obtain (complete) cathodic protection.

VI. CONCLUSION

The mechanism of the dissolution of aluminum in alkaline solutions has been discussed by a number of authors. Whenever an electrochemical mechanism is rejected (14) or modified (30), this is based on the assumption that impurities do not affect (or only to a slight extent) the rate of

dissolution. However, various forms of electrochemical mechanisms have also been suggested based on studies of the accelerating effects of impurities (2, 10), polarization measurements (2, 20), and experimental and theoretical investigations of the "difference effect" (10, 21–23, 28). Müller (10, 21) has interpreted the electrochemical observations in terms of his pore theory. According to Straumanis and Brakšs (2), the dissolution of aluminum in alkaline solutions is governed by local cell action whose activity is limited by a film of $Al(OH)_3$. In the case of highest purity aluminum, this film does not inhibit dissolution because it is dissolved rapidly by excess sodium hydroxide, and local cell action determines the rate of dissolution. However, for aluminum containing impurities, local cell action is so great that the dissolution of the $Al(OH)_3$ film formed determines the rate of dissolution of the metal.

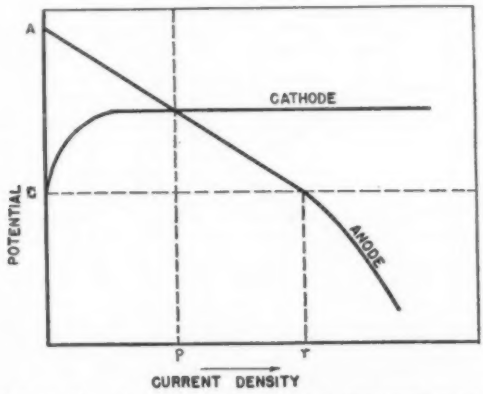

FIG. 16. Schematic polarization diagram for aluminum in solutions up to 0.5*N* sodium hydroxide.

The rate of dissolution of a metal when governed by an electrochemical mechanism is proportional to the effective potential difference of the local cells (determined by the open-circuit potentials and the polarization characteristics of the local anodes and cathodes) and the specific conductance of the solution. When the resistance of the solution is low and polarization effects are predominant, we may neglect the potential drop in the solution and represent the dissolution of alloy I in (less than 0.5*N*) sodium hydroxide by a schematic polarization diagram such as Fig. 16.[10] The influence of impurities accumulating on the surface on the electrode potential is excluded.

The electrode potential corresponding to a current density of p is the potential measured on aluminum dissolving without external current, and p is the local cell current. Increasing the current density by means of an

[10] Numerous examples of the development of such diagrams are given by Evans (27). The author is indebted to J. V. Petrocelli (private communication) for suggestions in connection with the development of this diagram.

external current while making aluminum the cathode does not change the electrode potential. When the current density is increased, while aluminum is made the anode, the electrode potential changes linearly in the cathodic direction. Hydrogen evolution on the anode is thereby gradually reduced until, at current density, r, it is suppressed entirely and the potential curve changes in slope at C. In the previous study (1) it was shown from considerations based on the theory of cathodic protection developed by Brown and Mears (25) that the limiting value of the "difference effect" is reached when the local anodes have been polarized to the open-circuit potential of the local cathodes.

As the concentration of sodium hydroxide is increased there is less anodic polarization at a given current density (Fig. 12 and 13) while cathodic polarization remains unaffected. Thus, as the concentration of sodium hydroxide is increased, the retarding effect of anodic polarization decreases and is probably reduced to a constant value in the range of 7 to 12N solutions, since the rate of dissolution in this range of concentration is directly proportional to the specific conductance of the solution.

This condition may be represented by the equation used in modified form by Ericson-Aurén and Palmaer (29, 31).

$$I = (E_1 - E_2)\frac{S}{C}$$

where I is the current density in all local cells, $E_1 - E_2$ the effective potential difference of the local cells (a function of the open-circuit potentials and the polarization characteristics), S, the specific conductance, and C, a constant depending on the form, arrangement, and size of the local anodes and cathodes. Thus, when the rate of dissolution (represented by I) varies directly with the specific conductance as the concentration of sodium hydroxide is increased, the polarization characteristics of the local anodes and cathodes must remain constant (assuming that C is constant).

ACKNOWLEDGMENT

The author wishes to express his thanks to Professor Gilbert E. Doan, Head, Department of Metallurgical Engineering, Lehigh University, for having made this investigation possible and to the Signal Corps Engineering Laboratories, Fort Monmouth, New Jersey, for permission to publish the information given in this paper. The author is also indebted to Mr. Bernt Roald, Lehigh University, for suggestions and discussions.

Any discussion of this paper will appear in the Discussion Section of Volume 96 of the TRANSACTIONS of the Society.

REFERENCES

1. M. A. STREICHER, *J. (and Trans.) Electrochem. Soc.*, **93**, 285 (1948).
2. M. STRAUMANIS AND N. BRAKŠS, *Korrosion u. Metallschutz*, **15**, 5 (1939).
3. G. TAMMANN AND F. NEUBERT, *Z. anorg. u. allgem. Chem.*, **201**, 225 (1931).
4. M. CENTNERSZWER, *Z. Elektrochem.*, **37**, 598 (1931).
5. R. GADEAU, L'aluminium raffiné in "Reine Metalle," p. 145, A. E. van Arkel, Julius Springer, Berlin (1939).
6. J. M. BRYAN, "Aluminium and Aluminium Alloys in the Food Industry," Food Investigation, Special Report No. 50, His Majesty's Stationery Office, London (1948).
7. J. M. BRYAN AND T. N. MORRIS, *J. Soc. Chem. Ind. London*, **59**, 159 (1940).
8. A. v. ZEERLEDER AND E. ZURBRÜGG, *Aluminium*, **20**, 365 (1938).
9. H. VOSSKÜHLER, *Aluminium*, **20**, 460 (1938).
10. W. J. MÜLLER AND E. LÖW, *Aluminium*, **20**, 257 (1938).

11. N. Isgarichew and W. Jordansky, *Korrosion u. Metallschutz*, **3**, 54 (1927).
12. E. Maass and W. Wiederholt, *Korrosion u. Metallschutz*, **5**, 265 (1929).
13. G. Schikorr, *Z. Elektrochem.*, **37**, 610 (1931); *Mitt. deut.* Materialprüfungsanstalt. S. **22**, 16 (1933).
14. M. Schenk, "Werkstoff Aluminium und Seine Anodische Oxydation," pp. 363-366 and 478, A. Francke Ag. Verlag, Bern, (1948).
15. J. K. Edgar, *Metals Tech.*, T. P. 2389, June, 1948.
16. W. L. Fink and L. A. Willey, in "Metals Handbook," 1948 Edition, p. 1161, A.S.M., Cleveland, Ohio.
17. "International Critical Tables of Numerical Data, Physics, Chemistry, and Technology," p. 247-254, McGraw-Hill Book Co., Inc., New York (1929).
18. S. Glasstone, K. J. Laidler, and H. Eyring, "Theory of Rate Processes," McGraw-Hill Book Co., Inc., New York (1941).
19. R. H. Brown, W. L. Fink, and M. S. Hunter, *Trans. Am. Inst. Mining Met. Engrs.*, **143**, 115 (1941).
20. J. V. Petrocelli and A. Phillips, *Trans. Electrochem. Soc.*, **85**, 257 (1944).
21. W. J. Müller, E. Löw, and F. Steiger, *Korrosion u. Metallschutz*, **15**, 1 (1939).
22. R. Piontelli, *Korrosion u. Metallschutz*, **18**, 346 (1942).
23. A. Thiel, *Z. Elektrochem.*, **33**, 370 (1927); A. Thiel and J. Eckell, *Korrosion u. Metallschutz*, **4**, 121 and 145 (1928).
24. M. A. Streicher, in "Pittsburgh International Conference on Surface Reactions," p. 105, Corrosion Publishing Co., Pittsburgh, Pa. (1948).
25. R. H. Brown and R. B. Mears, *Trans. Electrochem. Soc.*, **81**, 455 (1942) and **74**, 519 (1938).
26. B. P. Caldwell and V. J. Albano, *Trans. Electrochem. Soc.*, **76**, 271 (1939).
27. U. R. Evans, "Metallic Corrosion Passivity and Protection," Edward Arnold and Co., London (1946).
28. M. Straumanis, *Korrosion u. Metallschutz*, **14**, 67 (1938).
29. C. Wagner, in "Handbuch der Metallphysik," G. Masing, Band I, Teil II, Akad. Verlagsges, Leipzig (1940).
30. J. M. Bryan, *Chemistry & Industry*, p. 135, Feb. 28, (1948).
31. T. Ericson-Aurén and W. Palmaer, *Z. physik. Chem.*, **39**, 1 (1902), **45**, 182 (1903), and **56**, 689 (1906).

Addendum to:

CHEMICAL PROPERTIES OF THE INTERMETALLIC COMPOUNDS Mg_2Sn AND Mg_2Pb

by W. D. Robertson and H. H. Uhlig

Published in Volume 96, pages 27-42, July, 1949

The authors are indebted to the Office of Naval Research for support of this investigation on Contract No. Nr-ori-78 NR-031-187, T. O. 15.

A REACTION BETWEEN SOLIDS; THE FORMATION OF ZINC FERRITE FROM ZINC OXIDE AND FERRIC OXIDE[1]

D. W. HOPKINS

University College, Swansea, Wales

ABSTRACT

The formation of zinc ferrite, from a stoichiometric mixture of zinc oxide and ferric oxide, has been investigated from 600 C to 1150 C, with particular reference to the temperature of preparation of the ferric oxide. Under conditions which parallel those of roasting after removal of the bulk of the sulfur, there is a sharp decrease in the reactivity of the ferric oxide if the temperature of preparation exceeds about 675 C. There is no change in ferric oxide at this temperature, except for the Curie point at 678 C. The reaction is controlled by the diffusion of ferric oxide through the ferrite layer. The activation energies for the low and high temperature ferric oxides are 110,000 and 57,000 calories per mole respectively.

INTRODUCTION

This reaction is of considerable importance in the extraction of zinc by acid leaching of roasted sulfides, since zinc ferrite, $ZnO \cdot Fe_2O_3$, is insoluble in dilute mineral acids. Efficient recovery of zinc from ferruginous ores was not possible until the Tainton (1) process for the separation and strong acid solution of the compound was developed. The ferrite formation was found to be extremely sensitive to temperature, and, for this reason, reverberatory furnace roasting at 850 C or flash roasting at 950 C is still preferred to sintering, where the temperature may be 1350–1400 C. While virtually all the iron in sinter will be in the combined form, only about one third is combined in the products of the other roasting processes—about 35 per cent and 30 per cent in the case of ores containing the iron as pyrite. When the iron is present as marmatite, conversion to ferrite is practically complete, even under reverberatory roasting conditions.

Zinc ferrite formation has been the subject of investigation since 1851 (2), mainly for its effect on the efficiency of zinc extraction. Guillissen (3) found the minimum temperature of formation from the powdered oxides to be 580–600 C, when heated in air. Longuet (4) detected the compound in the coprecipitated hydroxides in water at 60 C, while Fricke and Dürr (5) found that zinc ferrite formed at 600 C from the oxides had a disordered lattice until heated to 700 C. Huttig (6) and Kittel (7) initiated a comprehensive investigation into the use of ferrites as catalysts for the oxidation of atmospheric nitrogen and determined the physical constants of a number of them. The magnetic properties were first examined by Wologdine (8) and further work is described in the publications of Snoek (9). The breakdown of zinc ferrite when heated in the presence of carbon has been investigated by Oldright (10) and later by Simon (11).

[1] Manuscript received April 1, 1949. This paper prepared for delivery before the Chicago Meeting, October 12 to 15, 1949.

This investigation is an attempt to determine the effect of the temperature of preparation of the ferric oxide on the rate of compound formation and to examine the mechanism controlling the rate within a given system of reactants.

RAW MATERIALS

High-purity zinc oxide and ferric oxide were further treated by solution in hydrochloric acid, filtration, and precipitation as the hydroxides. The precipitates were washed free from chlorides, as tested by silver nitrate, and were dried at 150 C in purified air. The zinc hydroxide was ignited at 500 C and stored in a desiccator with P_2O_5 and KOH. The ferric hydroxide was stored in a well-stoppered glass bottle and ignited in a platinum dish, as required, at the proper temperature. The batches of oxides were ground as near as possible to a common particle size and analyzed for impurities. The size distribution (Table I) within a batch was checked by reaction under standard conditions and unsuitable batches discarded.

TABLE I

	Zinc oxide	Ferric oxide
Analysis	Pure, with trace of CO_2	99.64% Fe_2O_3 + 0.32% FeO to 99.96% Fe_2O_3
Particle size	1.13 μ (one batch)	4.68–5.00 μ

EXPERIMENTAL PROCEDURE

Stoichiometric mixtures, containing 33.76% zinc oxide and 66.24% ferric oxide by weight, were prepared by mechanical mixing of the powders under conditions such that there was no further grinding. The ferric oxide was prepared at temperatures from 600 C to 1200 C by 50-degree intervals, except for the interval 650–700 C where additional samples were made at 10-degree intervals. The mixtures were heated in platinum dishes which were placed in the thermostatically controlled furnace at the appropriate temperature. For short-period treatments, the minimum weight of charge was used so as to reduce the heating-up time to about 30 seconds. At the end of the specified time, the charges were spilled onto a thick steel slab so as to cool them rapidly. Larger quantities were used for long periods, and samples were removed from the dish by a spoon.

ANALYSIS

The rate of combination was determined by estimation of the free zinc oxide remaining in a treated sample. As zinc oxide is soluble in ammoniacal ammonium chloride (Muspratt's) solution and zinc ferrite is not, except after a very long time of contact and at high temperature, the estimation was carried out in the following manner: a one-half-gram sample was leached in 70 ml of liquid containing 5 grams of ammonium chloride, 50 ml of distilled water, and 20 ml of 0.880 S.G. ammonia, at room temperature for 16 hours. The leach liquor and residue were washed into a Gooch crucible containing an asbestos pad which had been dried to constant weight. The residue remaining on the pad was washed with distilled water containing a few drops of ammonia and dried to constant weight at 1100 C.

The difference between this residue weight and the one-half gram represented the uncombined zinc oxide.

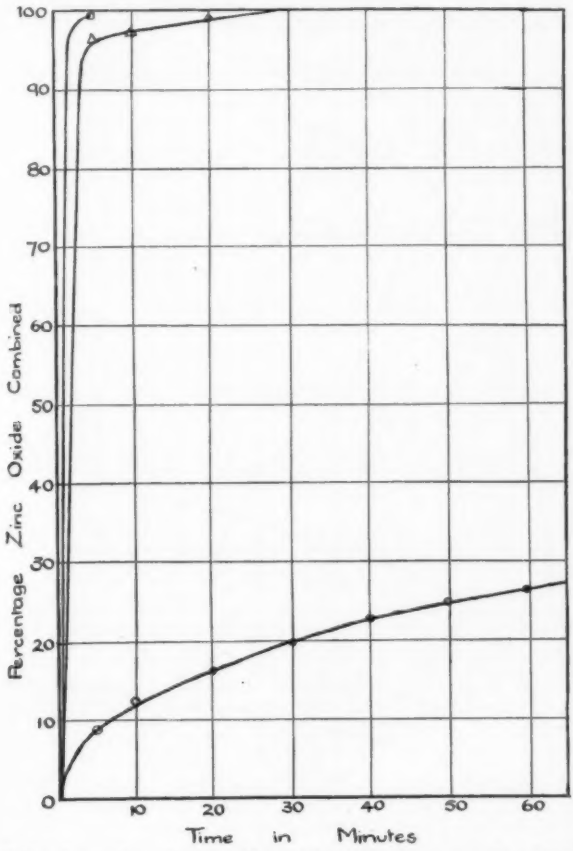

FIG. 1. Rate of reaction of zinc oxide and ferric oxide prepared at 650 C: ○——○ 600 C; △——△ 650 C; □——□ 700 C.

RESULTS

These are given in the form of tables and diagrams illustrative of the two major classifications into which the ferric oxide could be divided relative to its reactivity with zinc oxide. The division was according to whether the temperature of preparation was above or below about 675 C and the products of treatment at 650 and 850 C are given as typical of their respective classes.

DISCUSSION OF RESULTS

Preliminary examination of the results indicates that ferric oxide changes at about 675 C from an active to an inactive form relative to its reactivity with zinc oxide. The radical nature of the change is demonstrated by the diminution in the rate of combination to 10^{-3} times that obtained with

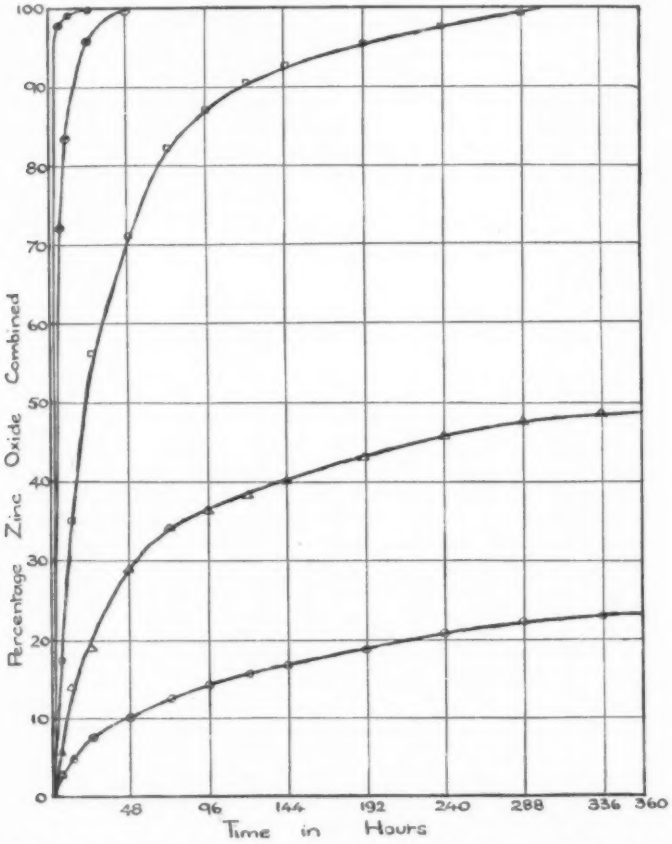

FIG. 2. Rate of reaction of zinc oxide and ferric oxide prepared at 850 C: ○——○ 650 C; △——△ 750 C; □——□ 850 C; ◓——◓ 950 C; ●——● 1050 C.

material prepared at temperatures below this value. There is also an effect of temperature between 850 and 950 C, but this is relatively small. The extreme sensitivity of the reaction to temperature is confirmed by the steep slope of the curve in both sections of Fig. 3. This last is a rough approximation to the formation of oxides from sulfides during roasting and their subsequent reaction at the same temperature.

The only change taking place in ferric oxide at temperatures near the value found is the loss of ferromagnetism at 678 C. Published data are emphatic on the continuity of x-ray spectrum, crystal habit, density, and diffraction pattern, over ranges of temperature well above and below this figure. According to Hedvall (12), a reaction taking place in the tempera-

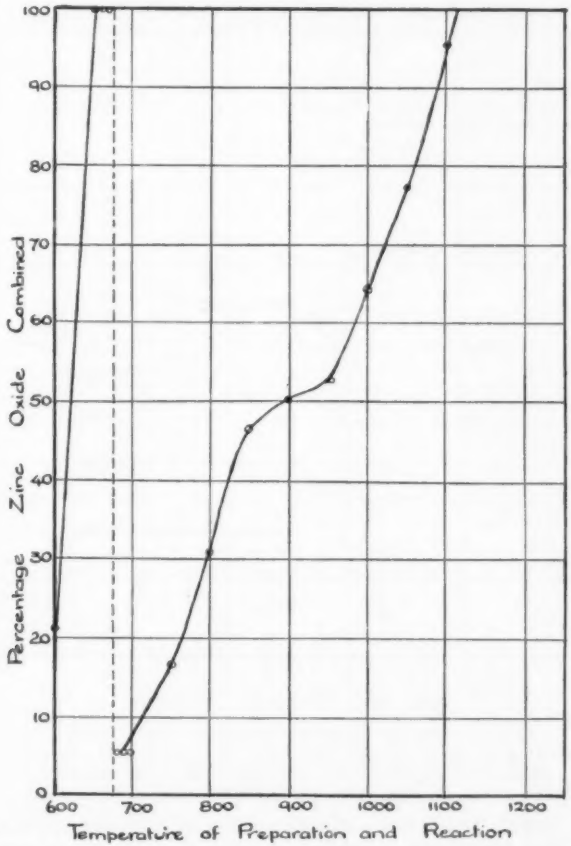

FIG. 3. Rate of reaction of zinc oxide and ferric oxide. Ferric oxide prepared and reacted at the same temperature.

ture range of a change, such as allotropic modification, should proceed with considerable velocity, but there is no evidence of this taking place. In fact, when mixtures with excess low-temperature ferric oxide were used for reaction at temperatures from 700 to 850 C, there was rapid initial reaction followed by very slow reaction with the ferric oxide that had been converted to the high temperature form during this time. The existence of "active"

ferric oxide is mentioned by Snoek, but no details of its preparation are given. Analysts have observed that ferric oxide which has been heated to temperatures given variously as "in excess of about 700 C" is very difficult to dissolve in acid, whereas the lower temperatures of ignition leave a readily soluble material. The possibility of reduction of surface area by sintering has been excluded by sizing analysis of the ferric oxide after

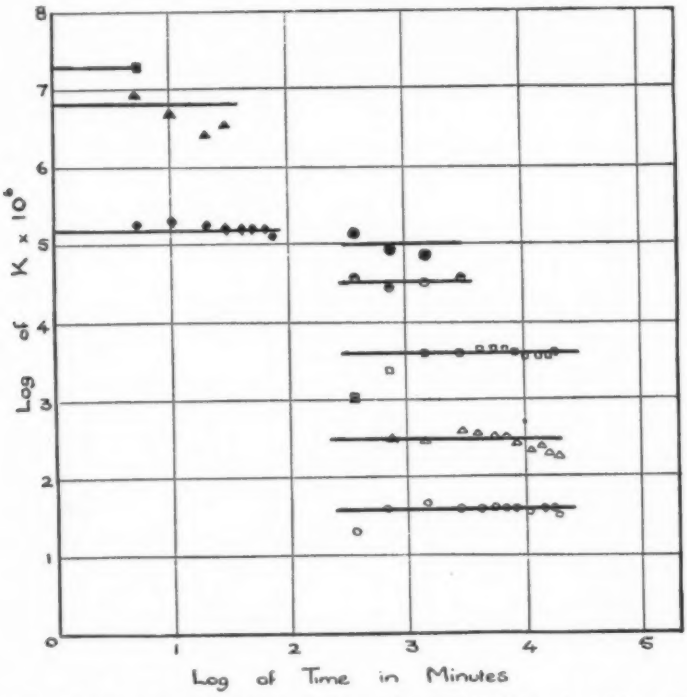

FIG. 4. Variation of K with time of experiment. "650" Ferric oxide at: 600 C ◆——◆; 650 C ▲——▲; 700 C ■——■. "850" Ferric oxide at: 650 C ○——○; 750 C △——△; 850 C □——□; 950 C ◓——◓; 1050 C ●——●.

heating to 700 C. This is not noticeably different from the low temperature material. The diminution in rate of increase of reaction velocity between 850 and 950 C can certainly be ascribed to sintering of the finer particles, although the temperatures are rather lower than the generally accepted range for sintering of ferric oxide. The mean particle size of a batch increased from 4.83μ to 5.16μ after reaction at 900 C for 30 minutes.

Reaction between solids is initially very rapid, due to the large number of points of contact, but the formation of an interposing layer of reaction product would quickly prevent further action unless one, or both, of the

materials was capable of diffusing through it. Any increase of temperature will increase the rate of reaction by increasing the speed of diffusion and chemical activity of the reactants. Since the effect of increase of temperature on the chemical activity is very much greater than the effect on diffusion speed, the latter will remain the rate controlling factor. Jander (13) and

TABLE II. *Reaction with ferric oxide prepared at 650 C*

Time in minutes	600 C	650 C	700 C
	$K(x10^{-2})$	$K(x10^{-2})$	$K(x10^{-1})$
5	1.80	9.1	2
10	1.85	5.0	
20	1.68	3.0	
30	1.73	3.3	
40	1.72		
50	1.66		
60	1.60		
70	1.40		
Weighted average.....	1.70	7.0	2

TABLE III. *Reaction with ferric oxide prepared at 850 C*

Time in minutes	650 C	750 C	850 C	950 C	1050 C
	$K(x10^{-3})$	$K(x10^{-4})$	$K(x10^{-4})$	$K(x10^{-4})$	$K(x10^{-3})$
360	2.25	10.0	1.13	3.3	1.47
720	4.0	3.33	2.50	2.8	0.87
1440	4.66	3.0	4.0	3.0	0.70
2880	4.16	4.0	4.0	3.5	
4320	4.16	3.84	4.5		
5760	4.32	3.33	4.33		
7200	4.16	3.16	4.16		
8640	4.0	2.84	4.0		
11520	3.84	2.25	3.67		
14400	4.0	2.37	3.50		
17280	3.84	2.16	4.0		
20160	3.33	2.0			
Weighed average.....	4.2	3.2	4.2	3	1

others have examined the theoretical characteristics of diffusion reactions and have derived a formula relating reaction rate to time which is a criterion of diffusion control:

$$Kt = \left\{1 - \sqrt[3]{\frac{100 - x}{100}}\right\}^2$$

K is a constant, t is time, and x is percentage reaction. K is related to temperature by the usual relationship $K = Ce^{q/RT}$, where C is a constant, depending on the physical nature of the reactants, T is the absolute temperature, q the heat of activation, and R the gas constant in calories.

In Tables II and III, values of K have been calculated according to this

formula for the two varieties of ferric oxide at the temperatures used. Because of the considerable range of values found and the great difference in the time scales, the logarithms of the values of K and the time in minutes have been used as abscissas in Fig. 4. This diminishes the scatter of values, so the tables are the better guide to the constancy of the values of K. Some of the findings must be approximate because of the very high reaction

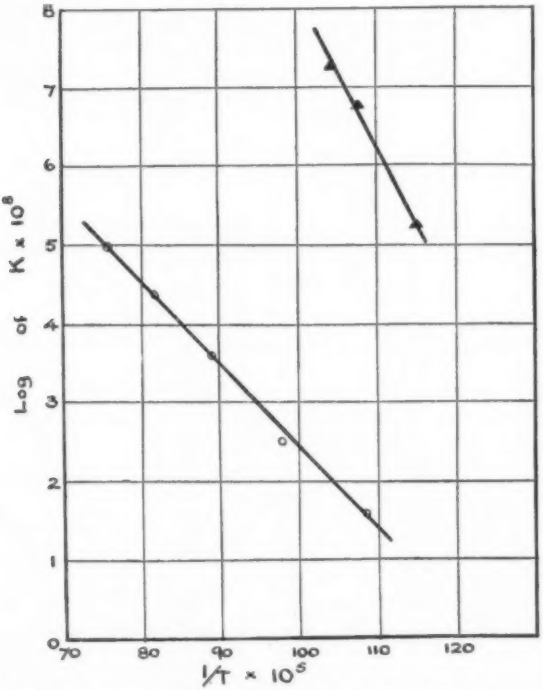

FIG. 5. Relation between log K and $1/T$. "650" Ferric oxide ▲——▲; "850" ferric oxide O——O.

velocities under certain of the conditions, but it will be seen that the criterion is satisfied for most of the experimental results. By plotting log K against $1/T$ it is possible to obtain an approximate value for the heats of activation. This has been done in Fig. 5. The values obtained are 110,000 cal/mole for the low temperature ferric oxide and 57,000 cal/mole for the high temperature variety. From the evidence of the solubility of ferric oxide in zinc ferrite at higher temperatures, it is concluded that this is the diffusing reactant.

Any discussion of this paper will appear in the discussion section of Volume 96 of the TRANSACTIONS of the Society.

REFERENCES

1. U. C. Tainton and L. T. Leyson, *Trans. Am. Inst. Mining Met. Engrs.*, **70**, 486 (1924).
2. E. Ebelman and G. Pelouze, *Ann. chim. phys.*, **33**, 53, 5 and 34 (1851).
3. J. Guillissen and P. J. Van Rysselberghe, *Trans. Electrochem. Soc.*, **59**, 95 (1931).
4. J. Longuet, *Compt. rend.*, **213**, 483, 577 (1941).
5. R. Frick and W. Dürr, *Z. Elektrochem.*, **45**, 3, 255 (1939).
6. G. F. Huttig, *Z. anorg. Chem.*, **210**, 26 (1933).
7. H. Kittel, *Z. anorg. Chem.*, **221**, 49 (1934).
8. C. R. Wologdine, *Compt. rend.*, **148**, 776 (1909).
9. J. L. Snoek, *Physica*, **3**, 463 (1936).
10. G. L. Oldright, *Tech. Papers Min. Met. Res. Utah* (1929).
11. A. Simon, *Z. Elektrochem.*, **8**, 53 (1940).
12. J. A. Hedvall, *Chem. Revs.*, **15**, 139 (1934).
13. W. Jander, *Z. anorg. Chem.*, **163**, 1 (1927); **166**, 31 (1927); **168**, 113 (1928); *Angew. Chem.*, **49**, 875 (1936).